FEDERAL UNIVERSITY OF CEARÁ

CENTER OF SCIENCE

PHYSICS DEPARTMENT

UNDERGRADUATE COURSE IN PHYSICS

CAIO CÉSAR RODRIGUES EVANGELISTA

PROBING BLACK HOLE SHADOWS

FORTALEZA

2024

CAIO CÉSAR RODRIGUES EVANGELISTA

PROBING BLACK HOLE SHADOWS

Undergraduate Thesis submitted to the Physics Course of the Center of Science of the Federal University of Ceará, as a partial requirement for obtaining the Bachelor Degree in Physics.

Advisor: Prof. Dr. Roberto Vinhaes Maluf

Co-advisor: Prof. Dr. Gonzalo Olmo

FORTALEZA

2024

Dados Internacionais de Catalogação na Publicação
Universidade Federal do Ceará
Sistema de Bibliotecas
Gerada automaticamente pelo módulo Catalog, mediante os dados fornecidos pelo(a) autor(a)

E92p Evangelista, Caio César Rodrigues.

Probing Black Hole Shadows / Caio César Rodrigues Evangelista. – 2024.
61 f. : il. color.

Trabalho de Conclusão de Curso (graduação) – Universidade Federal do Ceará, Centro de Ciências, Curso de Física, Fortaleza, 2024.
Orientação: Prof. Dr. Roberto Vinhaes Maluf.
Coorientação: Prof. Dr. Gonzalo Olmo.

1. Shadow. 2. Intensity Profiles. 3. Geodesics. I. Título.

CDD 530

CAIO CÉSAR RODRIGUES EVANGELISTA

PROBING BLACK HOLE SHADOWS

Undergraduate Thesis submitted to the Physics Course of the Center of Science of the Federal University of Ceará, as a partial requirement for obtaining the Bachelor Degree in Physics.

Approved on: 28/02/2025

EXAMINATION BOARD

Prof. Dr. Roberto Vinhaes Maluf (Advisor)
Universidade Federal do Ceará (UFC)

Prof. Dr. Gonzalo Olmo (Co-advisor)
Universidade Federal do Ceará (UFC)

Prof. Dr. Bruno Arderucio
Troy Univeristy (TU)

Prof. Dr. José Euclides Gomes da Silva
Universidade Federal do Ceará (UFC)

To you, fellow physicist that might be reading this.

ACKNOWLEDGEMENTS

> Do you feel like someone was left behind? Asks the reporter. Well, if there's someone, this would be myself, until now I was too hard on myself, with people around me, because of all the effort and dedication that I have put onto myself. All this time I've sacrificed many things within myself
>
> Ayrton Senna, 1988 interview in Suzuka - Japan

Writing these acknowledgments is certainly a different feeling from anything I've experienced so far, specially because at this exact moment that I'm writing this, it is only missing one chapter to finish this undergraduate thesis. It has been long journey so far.

I got accepted in the physics program at UFC back in early 2020, when just month after classes had started the Covid pandemic got in the way and all classes had to be interrupted for a few months until it was decided to adapt into the online format. I can still remember all the doubts about my future that surrounded my head during that time, the feeling of having to leave Fortaleza to go back to my parents house in the country side was almost like a definite goodbye to the dream of becoming a physicist. Hence, I would like to start out by thanking my both my parents, Marcelo Tadeu and Neyse Maria, as well as my grand parents and my uncle, Edson Evangelista, Maria Graziela and Leonardo Evangelista. I wouldn't be able to move to Teresina back in high school where I got a accepted in a NASA higschool program and decided that I would pursue a physics degree, neither I would have came to Fortaleza before the pandemic where I lived for that short time at grandparent's. I wouldn't be writing these words if weren't for you.

At first glance, this project sounded simply amazing to me, I thank for that Gonzalo J. Olmo, my advisor. Even when many problems got in the way and I couldn't believe much in myself, you still motivated. During the last year and a half of work together I always thought

that you believed in me, specially when proposing problems to solve that I on my own thought that I wasn't capable of doing so. I hope I can be as supportive and as capable as an advisor. Thank you for all discussions, commitment and support so far.

A great amount of what I currently know and how I think about physics is due to the influence of Saulo D. Reis, Carlos W. Paschoal, Roberto V. Maluf, J. Euclides, Humberto A. Carmona, André G.S. Landulfo, J. Soares. Past projects we used to work together, classes throughout my undergrad, and specially both hallway and Journal Club discussions made me develop my own way of thinking about physics. You have taught not only some of the profound mysteries in the universe, but at times, how to be a better human being. I wish to have your dedication in teaching.

A lot of my writing style is surely influenced by the period that I worked with Julia Jaccoud on the YouTube channel "A Matemaniaca por Julia Jaccoud". You taught me with a great amount of patience how to have a clean writing and how to effectively communicate my ideas to a broad audience, this will always be marked on my pens and papers.

Many late night discussions happened with Frederico Pedrozo and Arthur Paschoalotto, even I being the less experienced one among our group, you guys always cherished my ups and were the first to help me when things started to fall down the hill. All three of us never met in person and thousands of kilometres always separated us, but I do hope that our roads may cross some day.

Since I started my undergraduate research project, there are three people that always stood by me and became true friends along the way. Alana Carolina, Leandro Lessa and Adriel de Oliveira, you were some of the greatest supporters I've had when I wanted to leave for my Master's and when I wanted to quit.

I do believe some friendships are quite unique, and the friends I made during my degree definitely fit in that belief. João Macedo, Célio Rodrigues, Artur Soares, Luciano Ferreira, Gabriel Ribeiro, Alexandre Mendonça, you all more than anyone made a huge difference in the last year. Many times we had our disagreements, but as the saying goes, it always would end up in a pizza. You kept the memory of dreams and ambitions and I couldn't remember it. Even though we begin to separate to different countries and states soon, I hope that our friendship will last.

When talking about companionship and opportunities, the person that crosses my mind is Nickolas Aguiar. Some of the people listed in here I only met because you either

introduced me or because you incentivised me to participate in some physics conference or school. Physics has always been the glue that stick our conversations even when we were just talking about life worries or happy moments, your encouragement through my Master's application process really made a difference. I would always be thrilled when we started talking about organizing general relativity and quantum field theory in curved spacetimes events. Our long telegram calls are always a big pleasure.

In the same direction I wanted to thank the organizing committee of the Golden Wedding of Black Holes and Thermodynamics, namely, Nickolas Aguiar, Bruno A. Costa, Rafael Grossi, Ricardo Correa, Antonio D. Pereira and Daine Danielson. I was and still am the less experienced among us and you always made sure that I didn't feel belonging or capable of being part of what we did and what yet has to come. I can still remember how I felt part of something much greater than myself during that first week of December 2023.

“Eu só não quero significar.

Porque significar limita a imaginação”

(Manoel de Barros)

ABSTRACT

General Relativity(GR) is the theory of gravity that better describes how objects fall under the presence of strong gravitational fields. Describing body's trajectories in the presence of compact object, predicting gravity waves, and in particular, the existence of black holes. The observations made by the Event Horizon Telescope(EHT), about the black holes in the centre of the galaxy M87, and in centre of the Milk Way, Sgr A*, gave rise to a new era in testing black hole theory and GR itself by means of luminosity coming from electromagnetic radiation of the accretion disk. Theoretical analysis and General Relativistic Magnetohydrodynamics(GRMHD) universally agree on two facts: The existence of a photon ring, and a luminosity gradient descent caused by the light rays emiited by the accretion disk that intersect the event horizon(EH), and thus, don't ever get to the detector. Hence, forming a shadow. This undergraduate thesis aims to review because of the very few available test within GR, specially for black holes, it becomes extremely necessary the use of 'Shadowgraphy', e.g, have some better observational viability in astrophysical scenarios, through numerical simulations for light ray geodesics, i.e, the ray tracing protocol, as well as simulating the properties of the accretion disk by the intensity profile distribution functions, so that one can extract optical, geometrical and emission information of the accretion disk.

Keywords: shadow; intensity profiles; geodesics.

RESUMO

A Relatividade Geral(GR) é a teoria da gravitação que melhor descreve o comportamento de objetos na presença de fortes campos gravitacionais, descrevendo a trajetória de corpos na presença de objetos compactos, prevendo ondas gravitacionais e em particular, buracos negros. As observações feitas pelo Event Horizon Telescope(EHT), sobre os buracos negros no centro da galaxia, M87, e sobre um no centro da Via Lactea, Sgr A*, deram ínicio a uma nova era de testes sobre buracos negros e GR em si, por meio da luminosidade devido a radiação eletromagnética vinda do disco de acreção, i.e, uma sombra. Análises Teóricas e simulações de Magnetohidrodinâmica Geral Relativística(GRMHD) concordam universalmente em duas coisas: A presença de um photon ring, e de um gradiente descendente de luminosidade causada pelos raios de luz emitidos pelo disco de acreção que intersectam o horizonte de eventos e por consequência não chegam ao detector, formando uma sombra. O objetivo principal dessa tese de graduação é revisar que devido à pequena quantidade de testes de GR para buracos negros, se faz necessária o uso de 'Shadowgraphy', e.g, analisar a viabilidade observacional de tais objetos em contextos astrofísicos, por meio do desenvolvimento de simulações para os raios de luz, utilizando do protocolo de ray tracing de geodesicas do tipo luz e simulação das propriedades do disco de acreção através da análise dos perfis de intensidades, para assim extrair propriedades opticas, geométricas e de emissão do disco de acreção.

Palavras-chave: sombras; perfis de intensidade; geodésicas.

LISTA DE FIGURAS

CONTENTS

1 OBSERVING THE INVISIBLE DRAGON IN THE SKY

> One day in the year 1666 Newton had gone to the country, and seeing the fall of an apple, as his niece told me, let himself be led into a deep meditation on the cause which thus draws every object along a line whose extension would pass almost through the centre of the Earth.
>
> Voltaire

The subject of general relativity falls very naturally into how the gravitational field influences the behaviour of matter and how matter influences the gravitational field. Even though it might look subtle, there's a deep connection to geometry and how general relativity is a theory about the dynamics of the geometry of spacetime in which one of its consequences is gravity. As shown in (ROVELLI, 2021), Einstein's great idea was that Newtonian and special relativistic space and time are real physical entities, but they are effects of a dynamical variable that exists in the physical world: the gravitational field. The gravitational field is what determines the rate at which a clock ticks, or the separation between the ends of a rod, since atoms and moving parts of a clock interact with this field, thus, Minkowski spacetime that is described by η_{ab}, is nothing but an approximation of the gravitational field where its dynamics can be neglected, which makes the description of the gravitational field something much more general than simply the Minkowski spacetime, but rather a field that varies from point to point, namely, $g_{ab}(x)$.

This idea is based on two things, as discussed in (WALD, 1984), the first is that all bodies are influenced by gravity,i.e, all objects fall precisely in the same manner in the presence of a gravitational field. Since motion is independent of the nature of the bodies the paths of freely falling bodies define a preferred set of curves in spacetime just as in special relativity the paths in spacetime of inertial bodies define a preferred set of curves, independent of the nature of the bodies, and because the paths of inertial bodies in special relativity are geodesics of the spacetime metric, then by the last paragraph's discussion, the paths of freely falling bodies are always geodesics, but in a more general spacetime metric the gravitational field would not be exactly a field, but rather a deviation of the spacetime geometry from the one of special relativity. The second one, which is based on philosophical grounds, is Mach's principle, which says that

the matter in the universe should contribute to the local definitions of non accelerating frames of reference, which implies that the trajectories of bodies in a given gravitational field is locally indistinguishable from the trajectories of free particles viewed from an accelerated frame, and since accelerated frames seem to mimic the effects of gravity, at least locally, then understanding these features of gravity brings some value into comprehending in a physical description of gravitation.

Moreover, in this context Einstein proposed an observer independent theory, that described the properties and dynamics of spacetime, but that in more general cases it is described in terms of a curved spacetime metric, that is related to the energy-momentum tensor of matter, thus ascribing and accounting for the physical effects of the gravitational field by the Einstein's equations,

$$R_{ab} - \frac{1}{2} R g_{ab} = 8\pi T_{ab}. \tag{1.1}$$

When combined with the geodesic equation, yield not only a description of certain spacetime geometries, but also the trajectories of particles in that geometry. So given a derivative operator and a curve whose tangent vector is parallel transported along itself, then it satisfies the following expression,

$$T^a \nabla_a T^b = 0. \tag{1.2}$$

The affine parameterization is assumed, as discussed by (WALD, 1984). It is worth pointing out that this equation is only valid for the case of a pressureless or constant pressure everywhere of a perfect fluid, i.e, particle trajectories through spacetime do not carry any type of interactions between each other. Imposing these condition on the conservation of energy-momentum, yields exactly equation for geodesic motion above. So in a coordinate system, this equation simply becomes,

$$\frac{\mathrm{d}^2 x^\nu}{\mathrm{d}\lambda^2} + \Gamma^\nu_{\sigma\mu} \frac{\mathrm{d}x^\sigma}{\mathrm{d}\lambda} \frac{\mathrm{d}x^\mu}{\mathrm{d}\lambda} = 0. \tag{1.3}$$

Such that $\Gamma^\nu_{\sigma\mu}$ are the Christoffel symbols. Furthermore, back in 1915, (EINSTEIN, 1915) used this very formulation of GR to correctly compute the anomalous precession of Mercury's orbit and also how starlight could be deflected by a massive body, e.g the Sun, and

of course as a successful theory it showed a very natural agreement with Newton's theory in the Newtonian limit, in which either the gravitational field is weak, or there's a low velocities regime, or completely static gravitational fields.

As previously discussed, the essence of Einstein's equations is that the spacetime geometry influences matter and matter influences the spacetime geometry, as the famous quote by (WHEELER, 2000) goes: *Spacetime tells matter how to move; matter tells spacetime how to curve*.

However, there's no tensorial object that carries information about the curvature of spacetime in Einstein's equations, neither the Riemann tensor or the Weyl tensor are present in those equations, thus considering vacuum solutions,e.g, $T_{ab} = 0$, implies that the Ricci scalar will also be null, and hence $R_{ab} = 0$. But this only says that in the absence of matter the Ricci tensor vanishes, which is not a sufficient condition for flatness, thus, only the distribution of matter and energy are not sufficient to determine the gravitational field, so spacetime can also be curved in the absence of matter. More consequences of Einstein's equations and its details are discussed in simple language by (BAEZ; BUNN, 2005).

In this framework, general relativity is the most successful theory of gravitation so far, surviving not only its tests but also having experimental confirmation of predicted phenomena like gravitational redshift, the recent observation of gravitational waves by the LIGO collaboration and, in particular, the main theme of this thesis: black holes.

1.1 What are Black Holes?

Back in Newton's time, a natural philosopher, named John Michell presented the idea to the Royal Society of London that according to Newton's theory of gravitation, given a certain set of conditions, there could be a star with escape velocity that was higher than the speed of light, thus he concluded that the light emitted by this star would not have enough speed to propagate throughout space which means that after reaching a certain height it would return to the star's surface since it didn't have enough speed to escape it. Hence, characterising what would be called a dark star, in Michell's own words:

> *If there should really exist in nature any bodies, whose density is not less than that of the sun, and whose diameters are more than 500 times the diameter of the sun, since their light could not arrive at us; or if there should exist any other bodies*

> *of a somewhat smaller size, which are not naturally luminous; of the existence of bodies under either these circumstances, we could have no information from sight; yet, if any other luminous bodies should happen to revolve about them we might still perhaps from the motions of these revolving bodies infer the existence of the central ones with some degree of probability, as this might afford a clue to some of the apparent irregularities of the revolving bodies, which would not be easily explicable on any other hypothesis; but as the consequences of such a supposition are very obvious, and the consideration of them somewhat beside my present purpose, I shall not prosecute them any further*.

Later on, (LAPLACE, 1835) would get to the same conclusions and publishing his ideas on dark stars on his book, *Exposition du système du monde*. Even though this sounds like the popular idea of black holes, this description do not fit exactly in the picture, since in the dark star concept if light escaped, it could only escape by some maximum height, so an arbitrarily close observer would be able to see the light coming from the star as long as this arbitrary distance was something between the light's maximum height and the star's surface, whereas as it will be defined in the next chapter, for a black hole light wouldn't even be able to escape by any height.

This idea would remain the dark side of physicists shelf's for some time, until Einstein published his field equations, which would reach a German physicist in the Russian front, which would lead to the publication of the first solution of Einstein's field equations, by (SCHWARZSCHILD, 1999), in which he solved the equations to the most obvious application of the theory of gravity, which is for the gravitational field created by a star, which to a good approximation is spherically symmetric gravitational field and that for simplicity it can be assumed as static. Moreover, it is natural that the first concern is with the empty space region surrounding the gravitating body, thus, a vacuum solution.

Little had Schwarzschild knew that what he had discovered was the first black hole solution of general relativity, which even though it represented the most simple case of all, it contained the essential element that characterised every known black hole of general relativity, the existence of a frontier that defines a no-return region and that everything that crosses this frontier collapses at the black hole centre. However this revealed a somewhat shocking consequence which is that black hole have spacetime singularities, making them be considered non physical

solutions of Einstein's equations, until (PENROSE, 1965) showed that every black hole must have a singularity in its interior.

Furthermore, black holes needed to have something more than just a mathematical theory that described them, they needed an origin mechanism so that astronomers could look for them. The fact that biology does not prohibits the existence of unicorns, it does not mean that they truly exist. This origin mechanism was provided by (OPPENHEIMER; SNYDER, 1939), in which they shown that for sufficiently heavy stars when reaching all thermonuclear sources, it will continuously collapse due to its own gravitational contraction, forming at the end of its "life", a black hole.

Hence, what remains is to question and answer how would it be possible to observe black holes, since at a classical level they do not emit or reflect any light, as we shall see it now.

1.2 The Observation of Black Holes

Even air as invisible to the naked eye as it seems, it is still possible to observe hurricanes, and similarly to hurricanes, the quest for observing black holes should be sacked by looking for their effects, i.e, trajectories of other nearby objects, like if there are planets or stars orbiting something invisible or by observed gravitational effects, like lensing images.

The first suspect of a black hole was found by a varying source of X-rays, Cygnus X-1, which is a binary gravitational system composed of a heavy star and a black hole, in which that star's matter would be pulled over towards the black hole, which would lead to the formation of an accretion disk around the black hole, such that after some certain time, the disk would get to extremely high temperatures, thus emitting X-rays.

But that's obviously not the only suspect of a black hole. In the centre of the Milky Way galaxy, by observing the trajectories of stars in the Sagitarius A* region, there's an object with about four million solar masses concentrated in a radius of less than 17 light hours, this would turn to be the 2020 physics Nobel Prize, by (GHEZ, 2000; GHEZ, 2003; GHEZ, 2008) and (GENZEL, 1994; GENZEL, 1997). However, that is nothing more than indirect evidence of black holes, thus further evidence is needed.

1.2.1 Observing The Shadow of a Black Hole

A few years ago, the Event Horizon Telescope(EHT) reported observations of the nucleus of the galaxy M87 , in which it was achieved a angular resolution comparable to the expected size of a supermassive black hole, by combining the observations of eight telescopes, resulting in the very first photography of a black hole, as discussed by (EHT, 2019a; EHT, 2019b; EHT, 2019c; EHT, 2019d; EHT, 2019e), marking the beginning of a new era in the analysis of electromagnetic phenomena around compact objects and on testing general relativity.

Moreover, what is actually being observed is not the black hole on its own, but a bright ring-shaped lump of radiation surrounding a black central region of an estimated 6.5 million solar masses. The usual interpretation of this phenomena calls for a deviation of light rays in the gravitational field, of a black hole having a photon sphere, i.e, a critical unstable curve located at $r = 3M$, constituted of photons that either escape to infinity or fall into event horizon. Thus having the inner region bounded by the photon sphere, as the black hole shadow, since the photon sphere region is a bit larger than the event horizon region, that is located at $r = 2M$. The groundbreaking discovery presented in these seminal papers also allows tests of the background geometry using gravitational lensing and the richness of the physics behind the accretion disk around the black hole, indicating that a compact object as black hole having a critical curve and being illuminated by an accretion disk may yield a complex contribution to the total luminosity given by several light ray trajectories, but in formal manners, the critical curve can be defined as the light ray received by the observer that when traced backwards would have approached asymptotically a bound photon orbit.

As it will be discussed in further sections, for a Schwarzschild black hole, this determines a critical impact parameter $b_c = 3\sqrt{3}$, which is determined only by the background geometry on the impact parameter region. However, the optical appearance of compact objects doesn't depend only on the spacetime geometry, but also on the physical properties of the illuminating accretion flow, as it shall be discussed later.

2 THE ANATOMY OF BLACK HOLES

There is no space.

There is no time.

There are only light cones.

(FUENTES, 2013)

As previously mentioned, for a sufficiently massive, cold and spherical body, it is impossible for it to achieve hydrostatic equilibrium, and thus, it shall go into a complete gravitational collapse as shown by (OPPENHEIMER; SNYDER, 1939), hence having a remaining spacetime structure that of a black hole. Black holes are spacetime regions predicted by general relativity in its purest form, since they are made uniquely by curved space, time, and energy. In simple words, black holes are regions in which no physical body can escape, not even light. Thus defining a no escape limit region, an event horizon. In fact, this framework can be formally defined as given by (WALD, 1984) and (CARROLL, 2019). So, what we wish is to properly define what is a no escape region, even though this notion can not be fully captured by simply taking a black hole in a spacetime $(\mathscr{M}, g_{ab})$ to be a subset $A \subseteq \mathscr{M}$, such that $\forall p \in A$, $J^+(p) \subseteq A$, meaning in words that future causal structure of any region of any spacetime could be called a black hole, which makes that not only too general, but it is not what happens in nature. Hence, we must take a great care into the steps of defining a black hole.

Moreover, in asymptotically flat spacetimes, the impossibility of escaping to future null infinity can provide an appropriate definition of a black hole, which mainly distinguishes it from the causal future of any point in the Minkowski spacetime. Essentially what this means is that the causal past of future null infinity is nonsingular, but it does not include the whole spacetime, as for in the Minkowski spacetime, it does include the entire spacetime region. Hence the black hole formal definition goes as the following,[1]

Definition 2.1 (Black Hole) *Let $(\mathscr{M}, g_{ab})$ be an asymptotically flat spacetime, then a black hole will be a region of spacetime, such that $\mathscr{M} \nsubseteq J^-(\mathscr{J}^+)$, which makes the black hole region of spacetime*

$$\mathscr{B} = \mathscr{M} - J^-(\mathscr{J}^+) \tag{2.1}$$

Such that $J^-(\mathscr{J}^+)$ is the causal past of future infinity

[1] As mentioned by (WALD, 1984), the white hole region can be defined by replacing $J^-(\mathscr{J}^+)$ by $J^+(\mathscr{J}^-)$.

This very definition implies a limitation by a boundary, called the event horizon.

Definition 2.2 (Event Horizon) *The boundary of the black hole region, $\mathscr{H}$, will be lightlike surface, that forbids any timelike or lightlike particle of escaping towards infinity once reaching it. Hence,*

$$\mathscr{H} = \mathscr{M} \cap \dot{J}^-(\mathscr{J}^+) \tag{2.2}$$

where $\dot{J}^-(\mathscr{J}^+)$ represents the boundary of the spacetime region, $J^-(\mathscr{J}^+)$

These very two definitions are very general, and do not restrict themselves to any specific kind of black hole, which is the reason why they can become with more general kinds of black holes. These definitions will not be used through this thesis, they are mentioned and stated as tool to understanding and restricting the notion of a black hole into mathematical language.

We can turn our attention to specific black holes, in particular, the Schwarzschild black hole and body trajectories in it.

2.1 Schwarzschild Black Hole

As in the Newtonian regime, the most obvious application of Einstein's theory of gravity would be for the field created by the Earth or the Sun, e.g, any object that can be approximated reasonably to a spherical body, implying a spherically symmetric and static gravitational field. This makes thus natural that a first concern would be in how the empty region around the spherical object would behave, i.e, a vacuum solution. Hence, the spacetime metric of such region should be something that only depends on rotational invariant quantities, $\{r^2 = \mathbf{x}\cdot\mathbf{x},\ \mathrm{d}\mathbf{x}\cdot\mathrm{d}\mathbf{x},\ \mathbf{x}\cdot\mathrm{d}\mathbf{x}\}$. Therefore the metric can only have the following form,

$$ds^2 = -A(t,r)dt^2 + B(t,r)\mathbf{x}\cdot\mathrm{d}\mathbf{x}dt + C(t,r)(\mathbf{x}\cdot\mathrm{d}\mathbf{x})^2 + D(t,r)\mathrm{d}\mathbf{x}\cdot\mathrm{d}\mathbf{x} \tag{2.3}$$

Because we are dealing with a spherical scenario, $\mathbf{x}\cdot\mathrm{d}\mathbf{x} = rdr$. Thus, now the above equation can be rewritten as,

$$ds^2 = -A(t,r)dt^2 + B(t,r)dtrdr + \Big(C(t,r)r^2 + D(t,r)\Big)dr^2 + D(t,r)r^2d\Omega^2 \tag{2.4}$$

Thus, without any loss of generality, the above line element can be written as,

$$ds^2 = -A(t,r)dt^2 + \tilde{B}(t,r)dtdr + \tilde{C}(t,r)dr^2 + \tilde{D}(t,r)d\Omega^2 \tag{2.5}$$

Moreover, considering the transformation $dt \to \alpha dt + \beta dr$ and letting $\tilde{B}(t,r) = 2A\beta$, makes it possible to reduce the metric to only three free functions, but once again because of staticity, these functions actually turn out to only depend on the radius. Hence making the metric become the following,

$$ds^2 = -A(r)dt^2 + B(r)dr^2 + r^2 d\Omega^2 \tag{2.6}$$

2.1.1 Birkhoff's Theorem

In general, Einstein's equations form a non-linear system of partial differential equations, in which there are six independent functions. However, symmetries can help to diminish the number of independent functions. As given in the above equation, in static vacuum, the number of independent functions is reduced to only two. In order to fully specify the remaining two functions, it is worth to describe and prove Birkhoff's theorem, as given by (HAWKING; ELLIS, 2023).

Theorem 2.1 (Birkhoff's Theorem) *Any solution of the vacuum field equations in which the spacetime admits the $SO(3)$ group as the group of isometries, must be static and asymptotically flat.*

As shown before on the first chapter of this thesis, a vacuum solution implies a null Ricci tensor, which thus yields a null Ricci scalar. Since the spacetime metric looks like Eq.2.6, then the Ricci tensor, associated with the covariant derivative of our metric can be calculated by imposing the staticity condition, i.e, $B(t,r) = B(r)$ and that $B(r) = b^{-1}(r)$, resulting in the relation for the metric after some tedious calculations, that are given in detail in the following Mathematica notebook.

$$ds^2 = -A(r)dt^2 + \frac{1}{A(r)}dr^2 + r^2 d\Omega^2 \tag{2.7}$$

which thus implies that

$$g_{\mu\nu} = \begin{pmatrix} -\frac{1}{2}\partial_r^2 A(r) - \frac{\partial_r A(r)}{r} & 0 & 0 & 0 \\ 0 & -\frac{1}{2}\partial_r^2 A(r) - \frac{\partial_r^2 A(r)}{r} & 0 & 0 \\ 0 & 0 & -\frac{r\partial_r^2 A(r) + A(r) - 1}{r^2} & 0 \\ 0 & 0 & 0 & -\frac{r\partial_r A(r) + A(r) - 1}{r^2} \end{pmatrix} \tag{2.8}$$

and finally calculating the spherical component of the Ricci tensor results in,

$$\frac{r\partial_r A(r) + A(r) - 1}{r^2} = 0 \tag{2.9}$$

Hence resulting in,

$$A(r) = 1 + \frac{C}{r};\ \ C \in \mathbb{R} \tag{2.10}$$

At first sight this constant might look like it's arbitrary, however, when performing the Newtonian limit in this spacetime, it turns out that $C = 2M$, in the standard use of natural units of this thesis. Hence, resulting in following static and asymptotically flat line element,

$$ds^2 = -(1 - \frac{2M}{r})dt^2 + \frac{1}{1 - \frac{2M}{r}}dr^2 + r^2 d\Omega^2 \tag{2.11}$$

2.1.2 Geodesics in The Schwarzschild Spacetime

The main goal of this thesis is to build and compute the shadow of compact objects with numerical methods, in particular, the Schwarzchild black hole. In order to do that, it is first necessary to understand geodesics as a study subject.

As discussed back in the first chapter, the geodesic equation is given by Eq.1.3, which is obtained via the action,

$$S = \frac{1}{2}\int \mathrm{d}\lambda\ g_{\mu\nu}\frac{\mathrm{d}x^\mu}{\mathrm{d}\lambda}\frac{\mathrm{d}x^\nu}{\mathrm{d}\lambda} \tag{2.12}$$

Such that λ is the affine parameter. In our particular case, Eq.2.11 makes the action turn into the form,

$$S = \frac{1}{2}\int \mathrm{d}\lambda\ \Big[-A(r)\Big(\frac{\mathrm{d}t}{\mathrm{d}\lambda}\Big)^2 + B(r)\Big(\frac{\mathrm{d}r}{\mathrm{d}\lambda}\Big)^2 + r^2\Big(\frac{\mathrm{d}\theta}{\mathrm{d}\lambda}\Big)^2 + r^2\sin^2\theta\Big(\frac{\mathrm{d}\phi}{\mathrm{d}\lambda}\Big)^2\Big] \tag{2.13}$$

Thus, the conjugate momenta for each coordinate, respectively are $\Big\{A\frac{\mathrm{d}t}{\mathrm{d}\lambda}; B\frac{\mathrm{d}r}{\mathrm{d}\lambda}; r^2\frac{\mathrm{d}\theta}{\mathrm{d}\lambda}; r^2\sin^2\theta\frac{\mathrm{d}\phi}{\mathrm{d}\lambda}\Big\}$ Making it then possible to compute the Hamiltonian for particles moving in this geometry,

$$H = \frac{1}{2}\Big[-\frac{1}{A}p_t^2 + \frac{1}{B}p_r^2 + \frac{1}{r^2}p_\theta^2 + \frac{1}{r^2\sin^2\theta}p_\phi^2\Big] \tag{2.14}$$

Now it is straightforward to compute the conserved quantities for this Hamiltonian, which are p_t, since our metric is static, meaning that the energy is conserved, because $p_t = E$ and p_ϕ, because of the spherical symmetry. Also, p_ϕ turns out to be the angular momentum of particles, L, in this spacetime, implying that angular momentum is conserved. This can be also be checked by first principles through Killing fields.(See theorem B.1) Because $\xi^a = (\frac{\partial}{\partial t})^a$ is the static Killing field and $\psi^a = (\frac{\partial}{\partial \phi})^a$ denotes the rotational Killing field.

Thus,

$$E = -g_{ab}\xi^a u^b = A(r)\frac{\mathrm{d}t}{\mathrm{d}\lambda} \tag{2.15}$$

and

$$L = g_{ab}\psi^a u^b = r^2\frac{\mathrm{d}\phi}{\mathrm{d}\lambda} \tag{2.16}$$

Moreover, the Hamiltonian is also conserved with respect to the affine parameter, then $\frac{\mathrm{d}H}{\mathrm{d}\lambda} = 0$. Hence, for a constant Hamiltonian, there are two options of physical significance,

$$H = \begin{cases} 0 & \to \text{Light rays} \\ -1 & \to \text{Massive particles} \end{cases} \tag{2.17}$$

Once again, because of the spherically symmetric scenario, the particle's movement happens in any constant θ plane. For instance, choosing for the equatorial plane, $\theta = \dfrac{\pi}{2} \Longrightarrow \frac{\mathrm{d}\theta}{\mathrm{d}\lambda} = 0$. So, rewriting the Hamiltonian in terms of all the conserved quantities yields,

$$2H = -\frac{E^2}{A(r)} + B(r)\Big(\frac{\mathrm{d}r}{\mathrm{d}\lambda}\Big)^2 + \frac{L^2}{r^2} = \kappa \tag{2.18}$$

Such that κ is some constant that depends on which type of geodesic we are dealing with, so $\kappa = \{-1;0\}$. Furthermore, in the case of geometries that obey Birkhoff's theorem, we get to the equation,

$$\Big(\frac{\mathrm{d}r}{\mathrm{d}\lambda}\Big)^2 = E^2 - A(r)\Big[\frac{L^2}{r^2} - \kappa\Big] \tag{2.19}$$

It is quite immediate to notice that the above equation looks like an equation for trajectories of particles under a effective potential of the form, $V_{\text{eff}} = A(r)\Big[\dfrac{L^2}{r^2} - \kappa\Big]$.

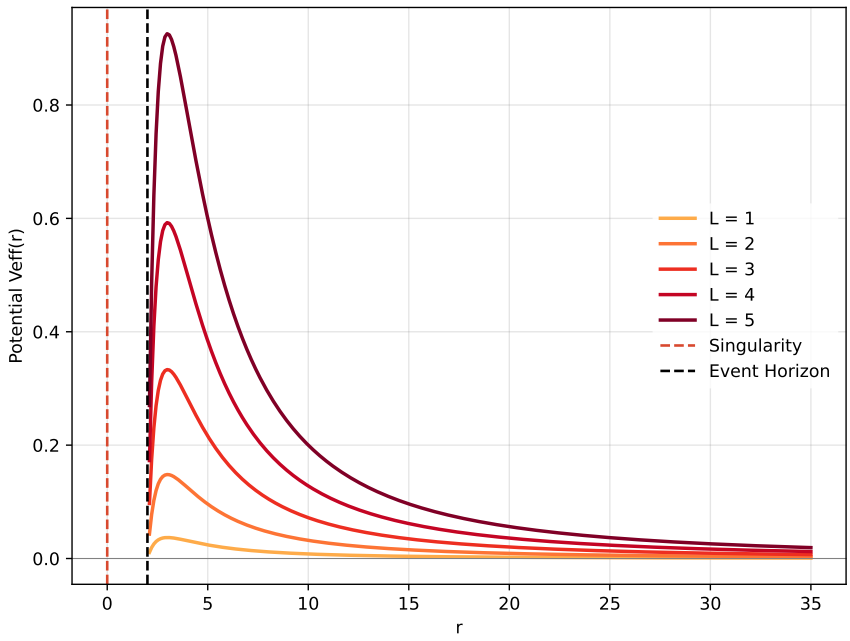

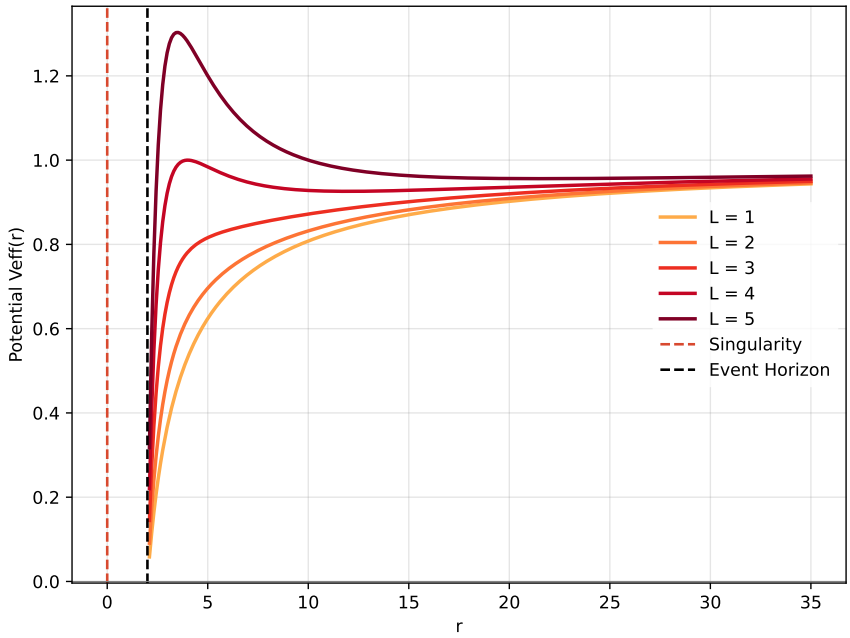

Figure 1 – The figure on the right represents the effective potential for photons, as for the the figure on the left represents the effective potential for massive particles. Both considering different values of angular momentum. At infinity, the effective potential goes to zero for the photon case, meanwhile, for massive particles it reduces to the non-relativistic case.

By taking a look at both forms of the potential, a reasonable thought is to analyse the stable and unstable trajectories, within the regions of spacetime given by it, and thus a glance at how the orbits behave in the framework of the Schwarzchild spacetime.

Furthermore, for massive particles in this spacetime we follow (WALD, 1984) discussion,

$$V_{\text{eff}} = \left(1 - \frac{2M}{r}\right) + L^2\left(\frac{1}{r^2} - \frac{2M}{r^3}\right) \tag{2.20}$$

So, the crucial new feature of general relativity, is the appearance of a new term, $-\frac{2M}{r^3}$ in the effective potential, which will play a much more significant role than the Newtonian and centrifugal terms for small radius, i.e, strong gravity regions.

Due to the fact that the potential has the above format, then there might be regions in which particles can have stable orbits. Thus,

$$\frac{\mathrm{d}V_{\text{eff}}}{\mathrm{d}r} = \frac{2M}{r^2}\left(\frac{L^2}{r^2} + 1\right) - \frac{2L^2}{r^3}\left(1 - \frac{2M}{r}\right) = 0 \tag{2.21}$$

Hence, solving it for r, it has the roots,

$$r_{\pm} = \frac{L^2 \pm (L^4 - 12L^2M^2)^{\frac{1}{2}}}{2M} \tag{2.22}$$

In this manner, if $L^2 < 12M^2$, there are no extrema for the potential, thus a particle with such amount of angular momentum and heading towards the centre of attraction, will inevitably fall into $r = 2M$ and then heading into a deep dive towards the spacetime singularity, at $r = 0$. On the other hand, for $L^2 > 12M^2$, it results that r_+ will be a minimum of the potential, while r_- represents a maximum of it. Because of that, unstable circular orbits will happen for $r \leq r_-$. Meanwhile, the potential minimum yields that any $r \geq 6M = r_{\text{ISCO}}$ are stable orbits, such that r_{ISCO} represents the inner most stable circular orbits, implying that any orbit with radii less than r_{ISCO}, are undoubtedly unstable circular orbits, although there might be non-circular orbits that extend into distances $r < r_{\text{ISCO}}$. Thus making $r_+ > r_{\text{ISCO}}$ and the unstable circular orbits domain ends up being restricted to the range

$$3M < r_- < 6M \tag{2.23}$$

This is illustrated in Fig.2.

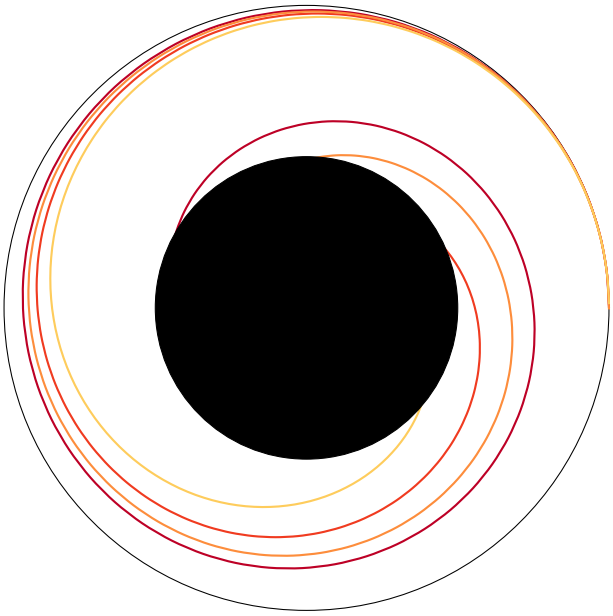

Figure 2 – Schwarzschild black hole with its ISCO orbit at $r = 6M$, showing that any timelike geodesic with radius $r < 6M$ ends up, in this case, falling into the horizon.

Additionally, because the main theme of this thesis is about black hole shadows, the geodesic case for light is of extreme importance, making it possible to analyse light deflection, gravitational lensing and image formation. The equation that describes the photon motion is

$$\frac{\mathrm{d}\phi}{\mathrm{d}r} = \pm\frac{L}{E}\frac{1}{r^2\left(1-\frac{A}{r^2}\left(\frac{L}{E}\right)^2\right)^{\frac{1}{2}}} \tag{2.24}$$

From the above equation, it becomes quite useful to define a numerical quantity to work with instead of all the variables in there, and that is so for two reasons. First, because angular momentum and energy are the two conserved quantities throughout the geodesic motion, then it makes sense to define something as their ratio, $b = \dfrac{L}{E}$, the impact parameter which has units of mass, and second, in our case of interest that will be discussed in the next chapter, this equations can only be solved by means of numerical methods. Therefore the equation becomes,

$$\frac{\mathrm{d}\phi}{\mathrm{d}r} = \pm\frac{1}{\left(\frac{r^4}{b^2}-r^2A\right)^{\frac{1}{2}}} \iff \frac{\mathrm{d}r}{\mathrm{d}\phi} = \pm\left(\frac{r^4}{b^2}-r^2A\right)^{\frac{1}{2}} \tag{2.25}$$

Moreover, by taking a closer look at the photon's effective potential in its extremum, we get to

$$L^2(r-3M) = 0 \tag{2.26}$$

Therefore, $r = 3M$ represents a circular orbit made out of photons, the photon sphere, which due to the fact that it sits right at a maximum of the potential, it is a unstable orbit. Furthermore, the ISCO represents a important role in black hole imaging, marking the inner edge of the accretion disk that surrounds the black hole, which can be seen from the famous black hole picture taken by (EHT, 2019a; EHT, 2019b; EHT, 2019c; EHT, 2019d; EHT, 2019e), however, the light actually should emerge from the photon sphere, since the light emitted from the accretion disk is extremely warped, what actually is there ends up being different from what is observed and because current telescopes don't have the resolution to observe the photon sphere, which makes impractical to observe if focussing effects are dominant in the light emitted by non-rotating black holes. This is illustrated in Fig.3

Considering again the Eq.2.18, in the limit for extremely large radius, that reduces to $\left(\frac{\mathrm{d}r}{\mathrm{d}\lambda}\right)^2 = E^2 \Longrightarrow r = r_i \pm \lambda E$, which is simply the definition of the Minkowski light cone with vertex at $r = r_i$. For instance, $r = r_i - \lambda E$ describes ingoing geodesics, since r diminishes as λ increases. However, outside this limit there's a region where the potential term is non-negligible, making the light cone get deformed. Furthermore, given that $\left(\frac{\mathrm{d}r}{\mathrm{d}\lambda}\right)^2 \geq 0$, at some instant λ_0, there is a an r_0, for which, $\left(\frac{\mathrm{d}r}{\mathrm{d}\lambda}\right)^2 = 0 = E^2 - \frac{AL^2}{r_0^2}$, and then the affine parameter evolution will make the radius to grow again, thus, r_0 must be a minimum, making the interpretation of the term $\frac{AL^2}{r^2}$ as a potential useful.

In practice, the photon trajectories will depend on the impact parameter, so noting that the maximum value of the potential is

$$V_{\mathrm{eff}}(3M) = \frac{b^2}{\sqrt{27}} \tag{2.27}$$

Combining with Eq.2.19 for the photon case, makes it possible to classify the photon trajectories in two possibilities. In the case for, $b_c < b$, the energy of light is lower than the angular momentum barrier, meaning that for radius $r < 3M$, the light emitted will not be able to escape to infinity, rather, it will orbit the black hole for a while and then fall into it, as in the other hand, for light rays coming from infinity will just bounce off the angular momentum barrier and be scattered back to infinity. For the opposite case, $b_c > b$, the energy of light is now greater than the angular momentum barrier, meaning that for light emitted at any $r < 3M$, can now escape to infinity, of course this only true for light emitted in the region $r_s < r < 3M$. As for the light coming from infinity, it is captured by the black hole and go all the way to $r = 0$.

In this setting, the maximum approximation of the deflected light rays happens when

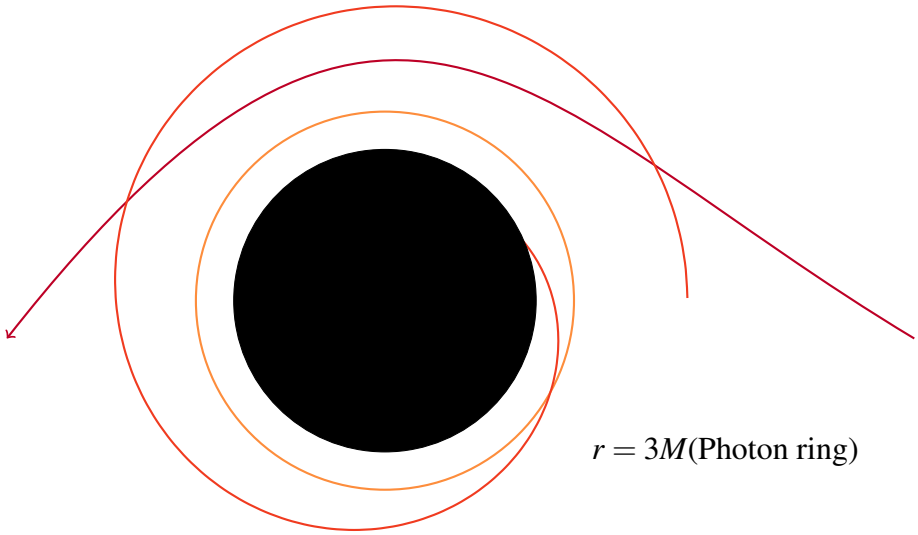

Figure 3 – Black hole represented with its photon ring at $r = 3M$, showing that a light ray that has a radius larger than $3M$ does not form a stable orbit.

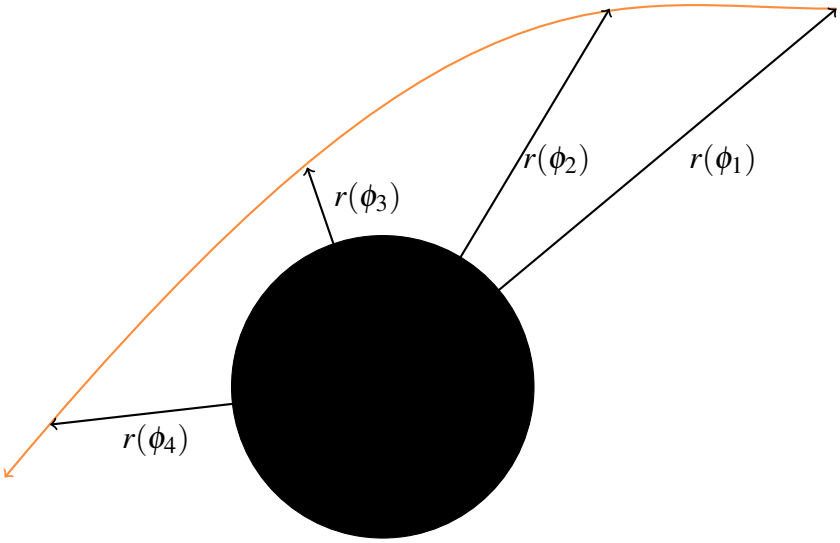

Figure 4 – Light ray coming from infinity towards the black hole with some definite impact parameter. It starts its trajectory with some angle ϕ_0, at a radius respective to the centre black hole, $r(\phi_0)$, such that as the trajectory goes on, the angle increases while the radius diminishes, until the minimum radius is reached and the radius starts to grow as the angle grows.

Eq.2.25 equals to zero, implying a impact parameter of the form $b^2 = \dfrac{r_{\text{min}}^2}{A(r_{\text{min}})}$.

Hence, from Fig.4 it makes sense to go with the convention that for light rays from infinity at some definite angle will assume the negative sign form of Eq.2.24. From the maximum approximation point, the angle keeps growing while now the radii also grows, thus implying that

from this point beyond, the light rays trajectory assume the positive sign form of Eq.2.24.

Furthermore, the complete light bending will be the sum of both contributions. For instance, in the simplest case, which is the absence of a gravitational field, $A(r) = 1$, the light deflection is

$$\Delta\phi = 2\int_{r_min}^{\infty} \frac{\mathrm{d}r}{\left[\frac{r^4}{b^2} - r^2\right]^{\frac{1}{2}}} = \pi \tag{2.28}$$

However, in the presence of gravity, in particular, in the Schwarzchild spacetime, $A(r) = 1 - \frac{2M}{r}$, and the angle deflection is $\Delta\phi = \alpha + \pi$. Thus, considering the substitution $v = \frac{r_{\min}}{r}$, Since, $b^2 = \frac{r_{\min}}{A(r_{\min})}$, then in the weak field limit $b \approx r_{\min}$. Thus the deflection angle integral becomes,

$$\alpha = 2\int_0^1 \mathrm{d}v \frac{1}{\left[1 - \gamma v^2(1 - \gamma v)\right]^{\frac{1}{2}}} - \pi; \;\; \gamma := \frac{2M}{b} \tag{2.29}$$

Because we are dealing with the weak field limit, it is straightforward to see that this limit only happens when $v \to 0$ and for values of $v_{\min} <<< 1$. On the other hand, for $M = 0$ the integral is easily solved turning into the previous case in which there was no gravitational field. Hence, we need to go through the contributions of high order in M, that are dominant for this. So expanding this integral for $\gamma \to 0$ terms, we find the light bending angle is

$$\alpha \approx \frac{4M}{b} \tag{2.30}$$

This means that within this perturbative approach, the particle escapes to infinity, at the angle given above. This is known as gravitational lensing and even though it is theoretically well understood there is a difficult in testing this prediction as mentioned by (TONG, 2013), since anything that goes behind the Sun is rarely visible. However, because the Sun and the Moon are approximately the same size as seen from Earth, it is possible to make those observations about stars whose light passes nearby the Sun, and then measure the star's positions on the sky. This measurement was historically carried out by Arthur Eddington and his fellows colleagues in Brazil in 1919. Also recently, (CRISPINO; LIMA, 2018) collected photos and documents of their official expedition to Brazil in which they made these observations.

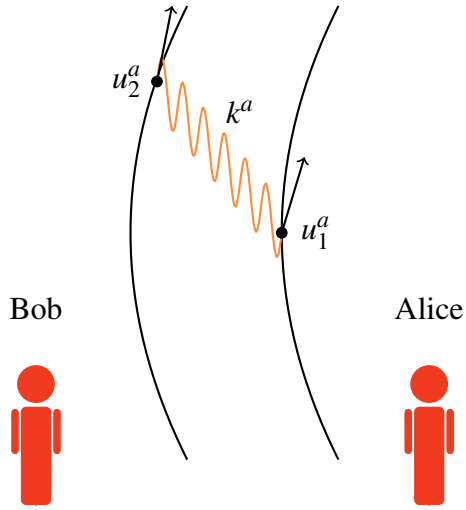

Figure 5 – Two static observers in the Schwarzschild spacetime, Alice and Bob. Alice sends a light signal to Bob that due to the gravitational redshift will be measured by Bob with a different frequency than Alice's.

2.1.3 Gravitational Redshift

Change in measured frequency by different observers is very known effect ever since Newtonian physics, with the non-relativistic version of the Doppler effect, as well as its relativistic version in SR settings. See (D'INVERNO; VICKERS, 2022) for more discussion on this.

A similar effect is the so called gravitational redshift, which has been measured and found to be in a agreement with prediction of general relativity to within 1% experimental deviation by (POUND; REBKA, 1959; POUND; REBKA, 1960), in which they monitored frequency shift in γ-rays as they fell on the surface of the Earth, by using the Mössbauer effect. As a consequence of this, gravitational time dilation and the equivalence principle would also need to hold, since clocks at different heights would have different rates in the presence of Earth's gravitational field.

Moreover, theorem B.1 and preposition B.1, must allow us to derive a formula for the change between emitted and observed frequency of light signals between two static observers, which by definition must be the gravitational redshift effect.

For instance, considering two static observers as illustrated in Fig.5, Alice and Bob, with respective four-velocities u_1^a and u_2^a. If Alice emits a light signal at event P_1, it will propagate through spacetime and is received by Bob at event P_2.

Once again, the geometrical optics approximation allows one to treat the light signal as a null geodesics, with tangent vector k^a. Thus, the emission frequency sent by Alice is defined

as,

$$\omega_1 = -k_a u^a\Big|_{P_1}, \tag{2.31}$$

and the frequency measured by Bob, similarly is,

$$\omega_2 = -k_a u^a\Big|_{P_2} \tag{2.32}$$

It is immediate that the tangent vectors for Alice and Bob at the respective events P_1 and P_2, point in the direction of timelike Killing vectors, ξ^a.

$$u_1^a = \frac{\xi^a}{\sqrt{-\xi^b\xi_b}}\Big|_{P_1}, \tag{2.33}$$

and

$$u_2^a = \frac{\xi^a}{\sqrt{-\xi^b\xi_b}}\Big|_{P_2}. \tag{2.34}$$

Hence, theorem B.1 and preposition B.1, $u^a\xi_a$ is a constant of motion along the light ray path, thus,

$$k_a\xi^a\Big|_{P_1} = k_a\xi^a\Big|_{P_2} \tag{2.35}$$

The norm of the static Killing field is $g_{ab}\xi^a\xi^b = A(r)$. Thus, the ratio between Alice's and Bob's frequencies is,

$$\frac{\omega_1}{\omega_2} = \sqrt{\frac{A(r_2)}{A(r_1)}}. \tag{2.36}$$

It is worth to notice that the above expression is only valid in stationary spacetimes, because of the dependence on the existence of a static Killing field on its derivation. In dynamical spacetimes such as Vaidya spacetime, due to the time dependency on the metric, it is not possible to have a well defined static Killing field and thus, the above expression can not be use for different geodesic observers in it. For more details on Vaidya spacetime See (LINDQUIST *et al.*, 1965; VAIDYA, 1951; COUDRAY; NICOLAS, 2021).

The frequency ratio equation implies that the radius in which Bob is located must be farther away from the black hole than Alice's, i.e, $r_2 > r_1$, which automatically makes $\omega_2 < \omega_1$,

meaning that the light frequency will be redshift, resulting in Bob measuring a light signal with less energy than Alice emitted it.

As final point on this, it is worth to point out that the maximum redshift of light from the surface of star, as mentioned by (WALD, 1984) is,

$$\frac{\omega_1}{\omega_2} = \frac{\omega(r = 9M/4)}{\omega(r \to \infty)} = 3 \tag{2.37}$$

,

Then the maximum redshift factor always is,

$$z = \frac{\omega_1}{\omega_2}\Big|_{\max} - 1 = 2. \tag{2.38}$$

Although this looks simple, it has significant consequences, as it rules out the possibility of any observed redshift of purely gravitational nature being greater than two.

2.2 Wormholes

Furthermore, the Schwarzchild solution in the form of $(2.1.9)$ ends its usefulness with all that has been discussed in the last section, however, it is only defined for radii $r \in (2M, \infty)$. Thus, because the radius of the event horizon does not represent a physical singularity and all radius in $r \in (0, 2M]$ should be considered, so a change of coordinates on the system becomes quite useful to explore more of the spacetime physics.

For instance, considering the region $r < 2M$, the Schwarzchild metric changes its sign, resulting in the spatial part becoming the temporal part and the temporal part becoming the spatial one. Performing a change of coordinates for this region,

$$ds^2 = -\mathrm{d}\rho^2 + a(\rho)\mathrm{d}z^2 + b(\rho)\mathrm{d}\Omega^2; \;\; a(\rho) = \frac{2M}{r} - 1, \; b(\rho) = r(\rho)^2 \tag{2.39}$$

The equation above is describing that in this region, the spacetime assumes some dynamics that depends on the ρ parameter. However, in the outside region, i.e, because spacetime is static, it is possible to exist static observers in it, as for the region described by the metric above, because every local point of spacetime depends on the dynamical parameter, there can be no static observers.

Moreover, by continuity, given the change of coordinates,

$$\mathrm{d}t = \mathrm{d}v - f(r)\mathrm{d}r \tag{2.40}$$

And the choice, $f(r) = A^{-1}(r)$, it results in the following metric that has no issues at $r = 2M$.

$$ds^2 = -A(r)\mathrm{d}v^2 + 2\mathrm{d}v\mathrm{d}r + r^2\mathrm{d}\Omega^2 \tag{2.41}$$

Following (HAWKING; ELLIS, 2023) discussion, in this procedure, cutting out the surface $r = 2M$ divides the spacetime manifold into two disconnected components for which $0 < r < 2M$ and the overlap region $2M < r < \infty$. However, because the spacetime manifold is connected, then a suitable choice for representing the external spacetime region is $r > 2M$, since even though the Schwarzschild metric is singular at $r = 2M$, no scalar of the curvature tensor diverges as r tends to $2M$, as shown bellow,

$$\lim_{r\to 2M} R_{\mu\nu\beta\alpha}R^{\mu\nu\beta\alpha} = \frac{3}{4M^4} \tag{2.42}$$

Suggesting that the singularity at the horizon is due to a bad choice of coordinates, so the spacetime manifold $(\mathscr{M}, g_{ab})$ can be extended, by first defining,

$$r^* = \int \mathrm{d}r \frac{1}{1-\dfrac{2M}{r}} = r + 2M\ln\frac{(r-2M)}{2M} \tag{2.43}$$

Which defines the $f(r)$ function in Eq.2.40, such that $f(r)\mathrm{d}r = \mathrm{d}r^*$. Then the advanced and retarded null coordinates are simply,

$$v = t + r^*; u = t - r^* \tag{2.44}$$

As discussed by (D'INVERNO; VICKERS, 2022), the congruence of radial null ingoing geodesics is given by constant v, which can be seen from the equation above.

Hence, using coordinates (v, r, θ, ϕ) the metric takes the so said Eddington-Finkelstein form, given by Eq.2.41. For this metric there is indeed no singularity at $r = 2M$, and it is analytic in the spacetime manifold for $0 < r < \infty$.

It is quite clear that within this larger spacetime manifold, the region $0 < r < 2M$, is isometric to that same region in the Schwarzschild metric. Hence, the act of picking up different

coordinate systems extends the Schwarzschild metric, such that now $r = 2M$ represents simply a null surface, i.e, it represents a section of spacetime with θ, ϕ constants such that the collection of points yield a two-sphere of area $4\pi r^2$.

Moreover, the Eddington-Finkelstein metric is not time symmetric because of the cross term, which comes from the fact that the $r = 2M$ null surface works as a one way membrane. since future directed timelike and null geodesics can only cross from $r > 2M$ into $r < 2M$ and never the opposite. Additionally, future directed timelike and null geodesics after crossing the event horizon surface approach $r = 0$ in a finite distance, even though the curvature scalar diverges as $r \to 0$, as it can be seen from Eq.2.42, indicating that $r = 0$ is a real singularity in the spacetime region. Therefore the spacetime manifold cannot be smoothly extended in $r = 0$.

For instance, considering the retarded coordinates (u, r, θ, ϕ) instead of the previous one, it results in,

$$\mathrm{d}s^2 = -A(r)\mathrm{d}u^2 - \mathrm{d}u\mathrm{d}r + r^2\mathrm{d}\Omega^2 \tag{2.45}$$

Which once again extends the spacetime manifold , since it is regular for $0 < r < \infty$ and $r = 2M$ still is a one way membrane null surface. However, because of the time reversal in the cross term as compared to the advanced Eddington-Finkelstein metric, it acts in the other direction of time, which is the reason as for why it is usually said this metric represents the spacetime of a white hole.

2.2.1 The Kruskal Coordinates

Furthermore, within this framework of the Schwarzschild solution, because the spacetime manifold is endowed with a metric geometry, then if every geodesic arising at some point in the spacetime, it can either be extended to infinite values of the affine parameter along the geodesic in both directions or terminates at an intrinsic singularity, then the spacetime manifold is said to be maximal. Thus, if a spacetime is maximal, then it is also said to be geodesically complete, although the converse is not true. For instance, because neither the Schwarzschild metric or the Eddington-Finkelstein extensions of it are not maximal, then there is a larger maximal manifold into which both advanced and retarded extensions can be, in such a manner that they coincide in the outer region, i.e, $r > 2M$, that is isometric to Schwarzschild. As shown by (HAWKING; ELLIS, 2023) and (D'INVERNO; VICKERS, 2022), such extension was given by Kruskal. In order to obtain it in $(\mathscr{M}, g_{ab}$, considering the coordinates (v, u, θ, ϕ), such that,

$$\frac{1}{2}(v-u) = r^* = r + 2M \ln \frac{r-2M}{2M} \tag{2.46}$$

Which induces the metric,

$$\mathrm{d}s^2 = -A(r)\mathrm{d}v\mathrm{d}u + r^2\mathrm{d}\Omega^2 \tag{2.47}$$

This metric defines a two-space, if θ, ϕ are constants, which in conformally flat coordinates yield a flat metric, $\mathrm{d}s^2 = -\mathrm{d}v\mathrm{d}u$. However, the most general coordinate transformation which leaves this two-space expressed in conformally flat coordinates is represented by two arbitrary C^1 functions, namely, $v' = v'(v)$ and $u' = u'(u)$. Then, we define the coordinates,

$$X' = \frac{1}{2}(v' - u'); \;\; T' = \frac{1}{2}(v' + u') \tag{2.48}$$

Thus, the metric takes the form,

$$\mathrm{d}s^2 = F^2(T', X')(-\mathrm{d}T'^2 + \mathrm{d}X'^2) + r^2(T', X')\mathrm{d}\Omega^2 \tag{2.49}$$

Leaving only the choice of v' and u' to fully determine the Kruskal metric. For instance, the choice Kruskal made was,

$$v' = e^{v/4M}; \;\; u' = -e^{-w/4M} \tag{2.50}$$

Because now the radial coordinate is a function of the primed Kruskal coordinates, then,

$$T'^2 - X'^2 = -(r-2M)e^{r/2M} \tag{2.51}$$

Hence, the Jacobian function of this transformation, F is given by,

$$F^2 = \frac{16M^2}{r} e^{-r/2M} \tag{2.52}$$

Substituting this into the Kruskal metric, results in the following,

$$\mathrm{d}s^2 = -\frac{16M^2}{r} e^{-r/2M}\mathrm{d}T^2 + \frac{16M^2}{r} e^{-r/2M}\mathrm{d}X^2 + r^2\mathrm{d}\Omega^2 \tag{2.53}$$

Moreover, in the spacetime defined by the Kruskal coordinates, the outer region defined by $X' > |T'|$ is isometric to that of Schwarzschild in which $r > 2M$, the region defined by $X' > -T'$ is isometric to the advanced Eddington-Finkelstein extension, as for the region defined by $X' > T'$, it is isometric to that defined by the retarded Eddington-Finkelstein. In a similar way, there is also a region defined by $X' < -|T'|$, which is geometrically identical to the asymptotically flat exterior Schwarzschild solution and is usually regarded as another asymptotically flat universe on the other side of the Schwarzschild throat. This can be more easily visualized in the following spacetime diagram of the Kruskal coordinates:

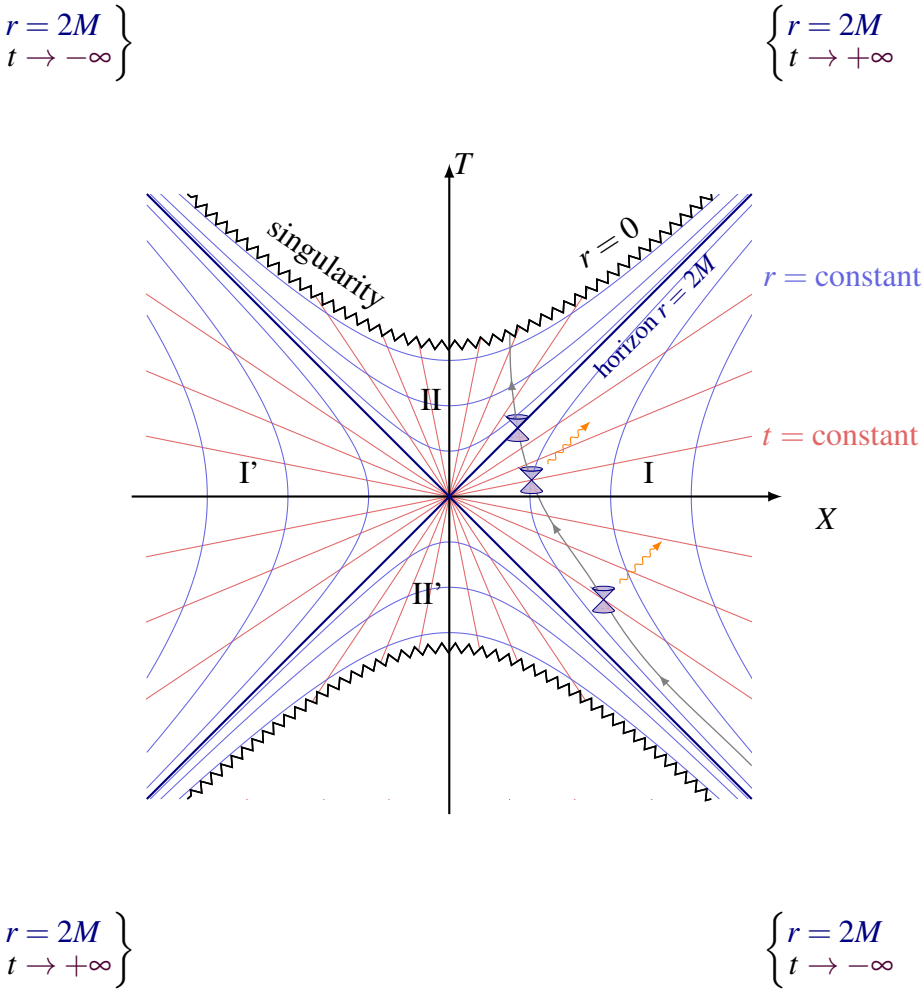

Figure 6 – Spacetime diagram representation of the maximal analytical extension of the Schwarzschild solution. The angular coordinates are suppressed. Region I is defined by $X' > |T'|$, which is asymptotically flat and isometric to $r > 2M$ of Schwarzschild. Region II, which is defined by $X' > -T'$, is isometric to the advanced Eddington-Finkelstein coordinates, and similarly the region II' is isometric to the retarded Eddington-Finkelstein coordinates. The region I' is asymptotically flat and isometric to the outer region of Schwarzschild.

This description illustrated Fig.6 of the Schwarzschild spacetime unravels many aspects of its causal structure, such as the fact that there are no timelike or null curves that can

cross the region I to I', as well as the fact that any future directed timelike or null curve that crosses the horizon, will eventually reach the singularity.

3 SHADOWGRAPHY

> Even for air, as invisible to the naked eye as it seems, it is still possible to observe hurricanes. And similarly to hurricanes, the matter of observing black holes should be worked by looking for trajectories of nearby objects.
>
> (LANDULFO, 2022)

In the usual common sense, a shadow can be classified in two different ways. The first, is simply a dark area on a surface, say the ground for example, caused by an obstacle that is located between a source of light and the surface in which one can see the shadow, it may be the shadow of a tree or a person next to a light post. The other one can be a dark silhouette of an object, observing only its shape and without the capability of seeing any of the object's details. In a similar manner, black holes can only be observed by their shadow, i.e, a dark silhouette caused by its own horizon, against a bright background that intrinsically depends on the gravitational bending of light, which seems to be the case as shown on the EHT observations in (EHT, 2019a; EHT, 2019b; EHT, 2019c; EHT, 2019d; EHT, 2019e). The term "black hole shadow" was first brought in a seminar paper by (FALCKE *et al.*, 2000), which for the first time discussed how it was possible to make black hole observations using interferometry methods. The theoretical problem of computing a black hole shadow can be formulated in many different ways, but they all agree that there is an observer very far away from the black hole, which must be close to light sources and that the observer has a "telescope" or a detector that collects all the light rays that don't reach the horizon or asymptotically escape in some different direction to infinity, that is later able to generate the image of a black hole.

Moreover, shadowgraphy is the process of computing light ray geodesics by means of Eq.2.24, in which initial data for the light ray radius and angle with respect to the centre of gravitational attraction are given, with a fixed constant of motion for each light ray path, the impact parameter. Thus, light ray paths can be classified by a single parameter, as it will be discussed, for certain range of values for the impact parameter, one can immediately tell if light falls into the horizon, has its trajectory deflected, produces a gravitational lensing effect or

if asymptotically approaches the unstable circular orbit, namely, the photon ring.[1] Afterwards, black holes in astrophysical scenarios will often absorb stars, cosmic dust or anything for the matter that they will accrete, thus creating a region in which there's an accretion disk around the black hole, which will be modelled by an intensity profile distribution, that is defined via general relativistic hydrodynamics or by simulations of the radiative transfer equation,

$$\frac{\mathrm{d}}{\mathrm{d}\lambda}\left(\frac{I_\nu}{\nu^3}\right) = \left(\frac{J_\nu}{\nu^3}\right) - \nu\alpha_\nu\left(\frac{I_\nu}{\nu^3}\right), \tag{3.1}$$

where I is the intensity, J the emissivity, α the absorptivity and ν, light's frequency.

This made possible the proposed result by (GRALLA *et al.*, 2020) as a parallel and powerful tool rather than general relativistic hydrodynamics. Which goes as,

$$I(r,\gamma,\mu,\sigma) = \frac{\exp\left\{-\frac{1}{2}\left(\gamma + \operatorname{arcsinh}\left(\frac{r-\mu}{\sigma}\right)\right)^2\right\}}{\sqrt{(r-\mu)^2+\sigma^2}}. \tag{3.2}$$

Since it is much less complex to work with analytic profiles that are capable of producing in certain physical scenarios as the same core predictions of general relativistic hydrodynamics.

Our goal in this chapter is to discuss and review, how to analytically compute the size of a black hole shadow, how numerical simulations of light ray geodesics work and how one can extract important physical data from then, and then by mixing the analysed data from the geodesics together with optical information from the intensity profile, compute black hole shadows.

3.1 The Shadow's Size

Before going through the general problem of computing a photograph of a spherically symmetric black hole surrounded by an emitting thin accretion disk, we must first concentrate efforts on the problem of light return on a black hole illuminated by a set of distant sources, say stars. This is an important first step, since the main characteristics from a geometrical optics approximation point of view, can be very illustrated in there.

Looking back at Eq.2.18 and considering the substitution, $u = 1/r$, we get for the angular Eq.2.24,

[1] Here, for static spherically symmetric scenarios photon ring and photon sphere are used indistinguishably

$$\left(\frac{\mathrm{d}u}{\mathrm{d}\phi}\right)^2 = 2Mu^3 - u^2 + \frac{1}{b^2}, \tag{3.3}$$

such that,

$$G(u) = 2Mu^3 - u^2 + \frac{1}{b^2} \tag{3.4}$$

So in order to analyse carefully and with more details than in Ch.**??**, we need to analyse the critical orbits for light rays, which mathematically means to solve the roots for $G(u)$ in the different cases that must be distinguished. Because when Eq.3.4 equals zero the problem is reduced to solving a third degree polynomial, then

$$u_1 + u_2 + u_3 = \frac{1}{2M} \tag{3.5}$$

and,

$$u_1 u_2 u_3 = -\frac{1}{2Mb^2}. \tag{3.6}$$

Moreover, the roots for $G(u)$ must allow negative real roots, and two others that can be real positive defined, which means that they can be coincident or not, and the last case is that they are simply a complex conjugate pair. For instance, by deriving the function $G(u)$,

$$G'(u) = 6Mu^2 - 2u = 0 \tag{3.7}$$

which only has two solutions, $u = 0$, or $u = 1/3M$, meaning that as $r \to \infty, u = 0$ and $r = 3M, u = 1/3M$. However, we must verify the condition for $u = 1/3M$ as a valid root. By substituting it in the $G(u) = 0$ equation, it results that $u = 1/3M$ is indeed a root if and only if,

$$b = 3\sqrt{3}M = b_c, \tag{3.8}$$

which is exactly the critical impact parameter as discussed back in Ch.**??**. For the case when the two positive roots coincide, i.e, $u_2 = u_3 = 1/3M \iff b = b_c$, then $u_1 = -1/6M$.

As we know, when the impact parameter admits a critical value, both Eq.3.3 and Eq.2.24 equal zero and a circular orbit of radius $r = 3M$, i.e, the photon ring is allowed as a null geodesic, even though this circular orbit cannot be stable.

Because we reduced the problem of critical orbits to the problem of solving a polynomial equation, we can rewrite Eq.3.3 in terms of its roots,

$$\left(\frac{du}{d\phi}\right)^2 = 2M\left(u+\frac{1}{6M}\right)\left(u-\frac{1}{3M}\right)^2. \tag{3.9}$$

Before going any further, we have once more showed that there exists a critical impact parameter, $b_c = 3\sqrt{3}M \approx 5.19695M$. On the other hand, it is clear that the rim of the optical black hole corresponds to rays which are marginally trapped by the black hole, i.e. they spiral around many times before reaching the observer, and in the Schwarzschild case which is what has been dealed with so far, this rim is exactly located at the critical impact parameter, as it will be formalized later on this chapter. From this, it is safe to say that the impact parameter can be viewed as a radius on the detector that a observer carries, so if Bob is an observer on Earth and he carries a photographic plate that detects all the light rays that didn't fell onto the horizon, at each point on the plate, there's an associated impact parameter. Thus for Bob, the apparent diameter of the black hole is about $10.95M$, as discussed by (LUMINET, 1979). This brief discussion is well illustrated in Fig.7.

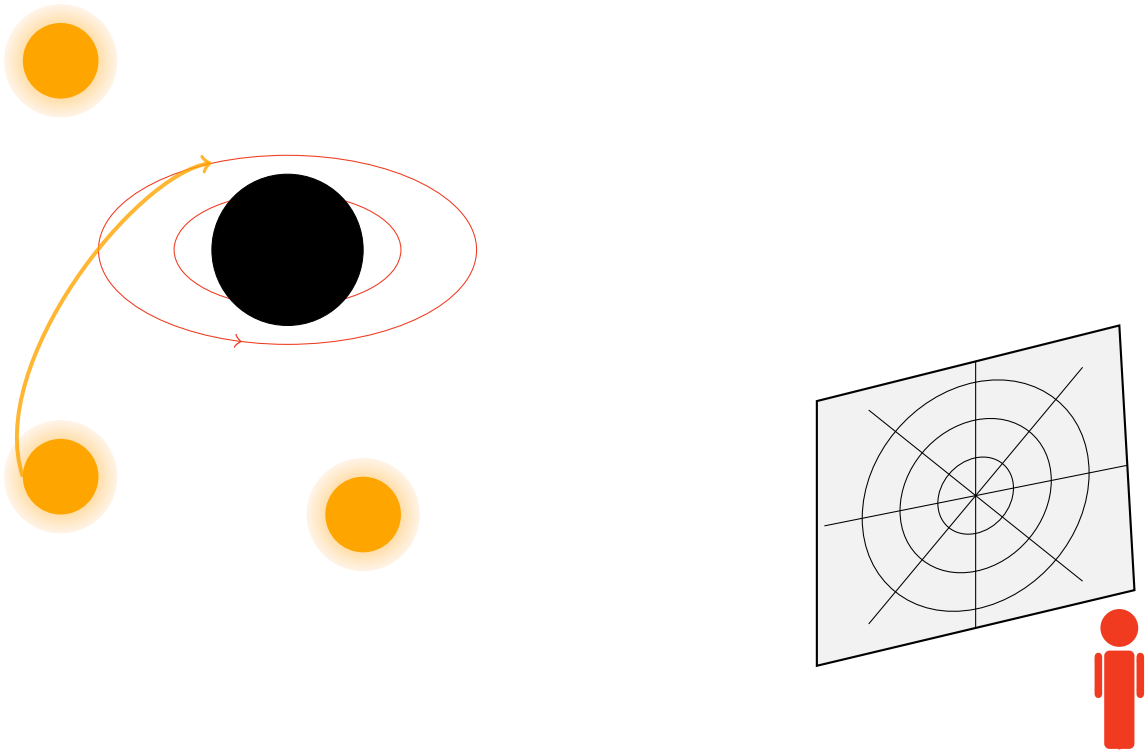

Figure 7 – A black hole surrounded by many sources of light, namely shinning stars, which all have some of their emitted light deflected and captured by the black hole, such that the deflected ones that reach the detector contribute to the photograph computation.

3.1.1 Impact Parameter Constraint

It is quite obvious that our main interest in this thesis is in the null geodesics that reach the observer's plaque, i.e. $b > b_c$. This family of geodesics posses a point of minimum radius, namely, a periastron, so it might be convenient to express all the quantities in terms of the periastron distance $r_{\min} = P$. Thus, let there be a quantity Q, such that,

$$Q^2 = (P-2M)(P+6M), \tag{3.10}$$

which makes now possible to express the roots of Eq.3.4 in terms of Q and the periastron.

$$u_1 = \frac{P-2M-Q}{4MP},\ u_2 = \frac{1}{P},\ u_3 = \frac{P-2M+Q}{4MP}. \tag{3.11}$$

From this we get that $u_1 < 0$, $u_2, u_3 > 0$ and $u_2 \neq u_3$, leading to a natural ordering of the roots, $u_1 < u_2 < u_3$, which requires the following inequality,

$$Q+P-6M > 0. \tag{3.12}$$

Once again by writing $G(u)$ in terms of its roots align with Eq.3.12, the impact parameter can now be thought in terms of the periastron.

$$b^2 = \frac{P^3}{P-2M}. \tag{3.13}$$

So given a value of P, we obtain the impact parameter at infinity measured on the plate detector. However, the converse is not true in a one to one correspondence. Given a certain impact parameter at infinity, because the above equation is not linear, it does not exist a unique minimum radius that corresponds to the given impact parameter. See (LUMINET, 1979; LUMINET, 2018).

Additionally, combining Eq.3.10 with the ordering inequality 3.12 and the above expression for the impact parameter, we conclude that $b > b_c$ is a constraint for the light rays with a periastron, which is exactly like we thought in the begging of this section and as discussed on Ch.**??**.

3.1.2 Cone of Avoidance

For constructing the shadow we'll start following (SYNGE, 1966), but for the case of a black hole. We can consider at fixed time, a cone of coordinates $(u,\theta,\phi),(u+\mathrm{d}u,\theta,\phi),(u,\theta,\phi+\mathrm{d}\phi)$, such that the half-angle of the cone is,

$$\cot\alpha = -\frac{1}{u\sqrt{A(u)}}\frac{\mathrm{d}u}{\mathrm{d}\phi}, \tag{3.14}$$

where $A(u)$ is the same function as that of Ch.**??** but considering $u = 1/r$. Substituting Eq.3.9 into the expression above and going back to radius coordinate r instead of u,

$$\cot\alpha = -\frac{1}{\sqrt{\frac{r}{2M}-1}}\left(1-\frac{r}{3M}\right)\sqrt{1+\frac{r}{6M}}, \tag{3.15}$$

or equivalently,

$$\tan\alpha = \frac{\sqrt{\frac{r}{2M}-1}}{\left(1-\frac{r}{3M}\right)\sqrt{1+\frac{r}{6M}}}. \tag{3.16}$$

What this is saying is that, by solving the angular equation, there is a well defined deflection angle, α, just as in Ch.2, that defines a cone generated by the null geodesics and light rays included in the cone must necessarily cross the horizon and get trapped. Hence, this cone of avoidance, or escape cone as described by (PERLICK; TSUPKO, 2022). At large distances, i.e. infinity, this cone must be described by a disk of radius $3\sqrt{3}M$, which is exactly the critical curve on the plate detector. Therefore, the cone must behave in such a way that at is narrow for $r > 3M$, opens up fully at $r = 3M$, and then for any $r < 3M$, it becomes directed outwards and becomes narrower as it approaches the horizon, where it is completely covered over, just as illustrated Fig.8.

Moreover, it is quite immediate that,

$$r\to\infty \Longrightarrow \alpha = \frac{3\sqrt{3}M}{r},\ r\to 3M \Longrightarrow \alpha = \frac{\pi}{2},\ r\to 2M \Longrightarrow \alpha = 0. \tag{3.17}$$

This agrees with the expressions found by (PERLICK; TSUPKO, 2022) in his review. So the angular size of the shadow measured by an observer at infinity with a detector plate is exactly that of the first expression from the above equation.

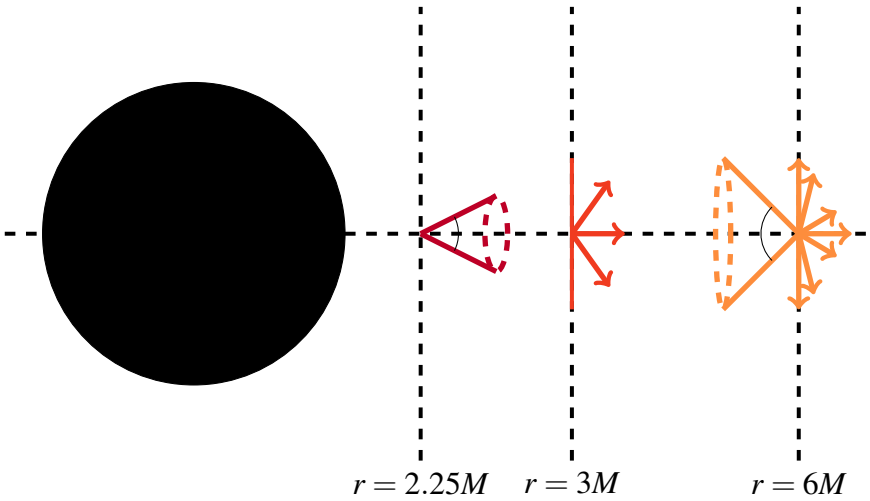

Figure 8 – The cone of avoidance behaviour for $r > 3M$, as a narrow cone, for $r = 3M$ completely open, and finally for $r < 2M$ narrowing again but outward directed. See figure 10 on (CHANDRASEKHAR, 1984) for comparison.

3.2 Ray-Tracing Protocol

Throughout this section the main goal is to reproduce the same results as (GRALLA *et al.*, 2019), which can be easily generalized to the black hole mimicker case as that of (GUERRERO *et al.*, 2021b).

The procedure of the ray-tracing protocol is quite simple as it goes back to the very formulation of the problem of computing the shadow of a black hole. Light rays are detected at an observers plate at infinity with a well defined impact parameter, and are traced back to the point of deflection in which they were originated, keeping in mind the presence of the strong gravitational field due to the presence of the black hole. This is all very well contained in Eq.2.24, which due to its chaotic behaviour can only be solved in all regions numerically.

Thus, for impact parameter values $b \in [b_c(1-2/10), b_c(1+2/10)]$[2], the null geodesics are traced in Fig.9.

As previously discussed, we are mainly interested in the class of null geodesics that are able to reach the detector, thus we consider next the following two ranges of impact parameter: $b \in [4b_c, b_c(1+1.9\cdot 10^{-1})]$ and $b \in [b_c(1+1.8\cdot 10^{-1}), b_c(1+6.2\cdot 10^{-1}]$, which can be seen in Fig.10

At this point, it is reasonable to figure out that this process continues iteratively for many different values of impact parameter, until we have the complete congruence of geodesics around the Schwarzschild black hole. It is worth to notice however that the total deviation of

[2] The impact parameter intervals throughout this thesis represent a initial impact parameter until a final one, such that $b \in [b_{\rm in}, b_{\rm f}]$.

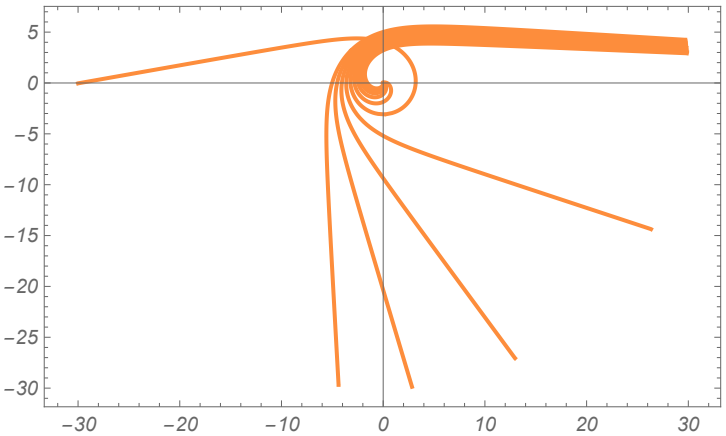

Figure 9 – Result of the numerical simulation for impact parameter values between the range $b \in [b_c(1-2/10), b_c(1+2/10)]$.

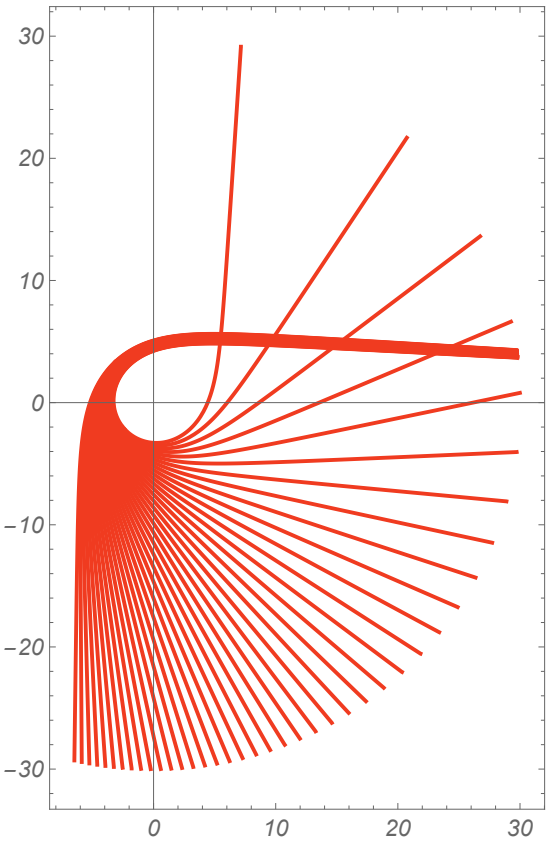

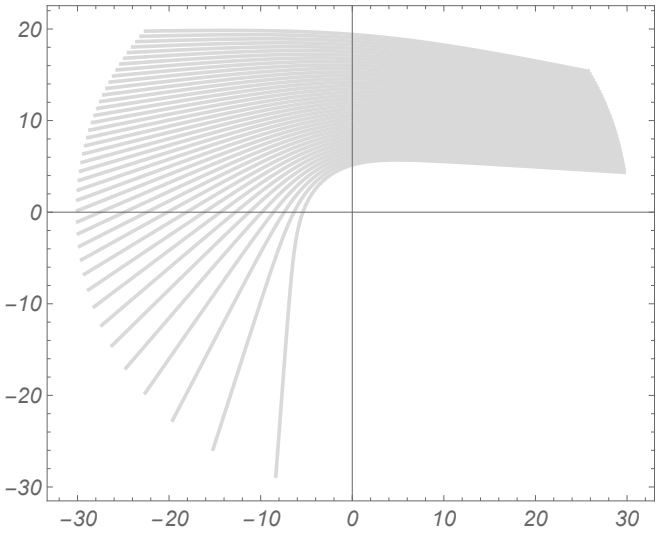

Figure 10 – The generated figure on the left shows interesting behaviour. Because there are photons going through the y-axes twice, i.e. going through the accretion disk twice, they form lensed rings around the black hole. What that means is that these photons are carrying luminosity intensity that comes from the front region of the accretion disk, but also from the back of the accretion disk, which causes the observer to see the back of the accretion disk. As for the one on the right, it simply represents weak deflection from the light rays are really far from the centre of gravitational attraction and how the deflection gets stronger as the light rays get closer to the black hole.

a light ray, α, given by, $\phi_\infty = \pi + \alpha$, and we already derived a formula for it at infinity, it is interesting to grasp some idea to what happens near the critical curve, i.e. b_c. The asymptotic expansion for the integral of Eq.2.24 leads to the following important relation.

$$b = b_c + 3.4823Me^{-\alpha}. \tag{3.18}$$

Furthermore, null geodesics that come off at some given angle α, include not only the exact family of the deflected angle itself, but also $\alpha + 2\pi$, $\alpha + 4\pi$, until $\alpha + 2\pi n$, where $n \in \mathbb{N}$. This means that as close as a light ray gets to the critical curve, its contribution should in principle be of higher order to the imaging, i.e. $b_\infty = b_c$. However, since,

$$b_n = b_c + 3.4823M\exp\{-(\alpha + 2\pi n)\}. \tag{3.19}$$

Astonishingly, what this is saying is that as the number of circuits around the centre of gravitational attraction increases, there is not only an infinite series contribution, but this infinite series contribution converges proportionally to a geometrical series, since $\sum_{n=0}^{\infty} e^{-2n\pi} = \frac{1}{1-e^{-2\pi}}$, which means that for the nth order contribution of a circuit around arbitrarily close the photon ring, it will only considerably contribute until $n = 2$ and successive circuits will add less intensity to the imaging around the photon ring. For a discussion in terms of cross-section see (LUMINET, 1979; THORNE *et al.*, 2000).

Finally, in its most pure state of art the geometrical characterization in terms of null geodesics is well expressed by Fig.11.

3.3 Intensity Profiles

Very compact objects, and thus, black holes, are usually surrounded by an accretion disk, i.e. an inflow of a hot gas spiralling slowly inward as it loses energy and angular momentum due to the gravitational attraction, and consequently in this process, emitting radiation. Differently from astrophysicists, we'll only consider physical scenarios where given certain balance of thermal pressure against gravity and rotation, the disk becomes geometrically thin or thick, which is equivalent to the approximation that the radial extension of the accretion disk can be much smaller or larger than its thickness.

Furthermore, the disk can provide several informations for the imaging and characterization of the black hole, for instance, to what extend it is transparent to its own radiation,

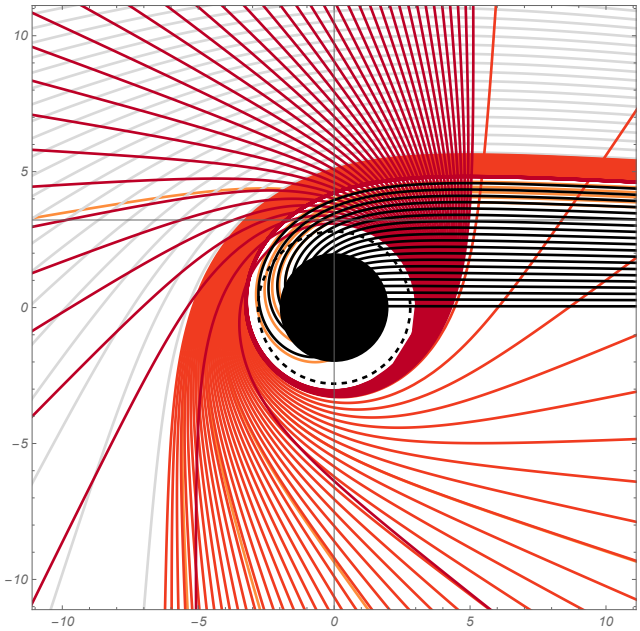

Figure 11 – The black hole is shown as solid disk with radius $r = 2M$ and the photon ring is expressed as a dotted circle located at $r = 3M$.

giving optical properties, the disk's shape, even though we'll only worry about geometrically thin or thick disks and last but not least, its emission properties, which will concern not only emission itself but also absorption and scattering in the disk. The last one is closely related to general relativistic hydrodynamics and its simulations via Eq.3.1, which we'll not worry because of the intensity profile distribution on Eq.3.2. It is worthy stating that in the intensity profile distribution provided, γ is related to the rate of intensity growth from infinity to its peak, μ shifts the profile and consequently its peak to desired locations, and σ, sets the dilation of the disk. Hence, there are two very unique and important characteristics of the intensity profile that come from the set of parameters and act in the generation of images, namely, the location of the peak intensity of emission and the decay with the distance, which are closely related to the shadow observables and the photon ring.

In the case in which the accretion disk is transparent to its emitted radiation, Liouville's theorem requires flux conservation, which yields that,

$$\frac{I_{\nu_0}}{\nu_0^3} = \frac{I_{\nu_e}}{\nu_e^3}, \tag{3.20}$$

where ν_0 is the frequency in the observer's frame and ν_e is the frequency in the emitter's frame, much like Alice and Bob scenario discussed in Ch.**??**. If for instance we let g be a redshift factor,

$$g = \frac{\nu_0}{\nu_e}, \tag{3.21}$$

then Eq.3.20 leads to, $I_{\nu_0} = g^3 I_{\nu_e}$. For the matter of simplifying our assumptions about the disk's emission behaviour, for a monochromatic emission in the disk frame in the whole frequency spectrum,

$$I_0 = \int d\nu_0 I_{\nu_0} = \int d\nu_e g^4 I_{\nu_e} = g^4 I(r). \tag{3.22}$$

Because the redshift factor at with the observer's located at infinity is well defined by Eq.2.36 and the Schwarzschild spacetime is a asymptotically flat one,

$$I_0(r) = A^2(r) I(r). \tag{3.23}$$

In complement, null geodesics arbitrarily close to the critical curve can circle around infinitely many times, even though contributions higher than second order tend to a minimum, it is useful to consider then for numerical accurate data treatment. Thus, the last equation becomes,

$$I_0(r) = \sum_{n=0}^{\infty} A^2(r) I(r). \tag{3.24}$$

For any further and detailed discussion on how higher order circuits and intensity profile computation, see (GRALLA *et al.*, 2019; GUERRERO *et al.*, 2021b; GUERRERO *et al.*, 2021a; OLMO *et al.*, 2023).

As a final point, we can plot the intensity profile distribution for different set of parameters, mainly,

$$I = I_{\text{ISCO}}(r, -2, 6, 1/4) \tag{3.25}$$

$$I = I_{\text{pr}}(r, -2, 3, 1/8) \tag{3.26}$$

$$I = I_{\text{EH}}(r, -3, 2, 1/8) \tag{3.27}$$

$$I = I_{\text{centre}}(r, 0, 0, 2) \tag{3.28}$$

Hence, when considering all the contributions to the imaging from the intensity profile and the correct data treatment taking gravitational redshift into account, we can compute the black hole shadow, for instance for the ISCO profile, as shown in Fig.13.

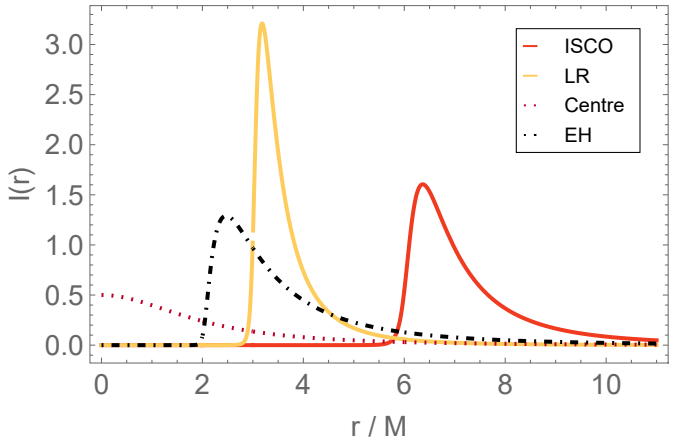

Figure 12 – Plot of different intensity profiles for different parameters. The ISCO profiles is referred as a profile with its peak around the ISCO radius if one treats the accretion disk an ensemble of timelike geodesics. The PR stands for photon ring, so one could simply consider a disk that extends itself until the photon ring. The EH stands for event horizon and is useful to model infalling matter of the disk in the horizon. The centre profiles stands for ultra compact objects with no horizon, so the accretion disk could extend itself up to the centre of gravitational attraction.

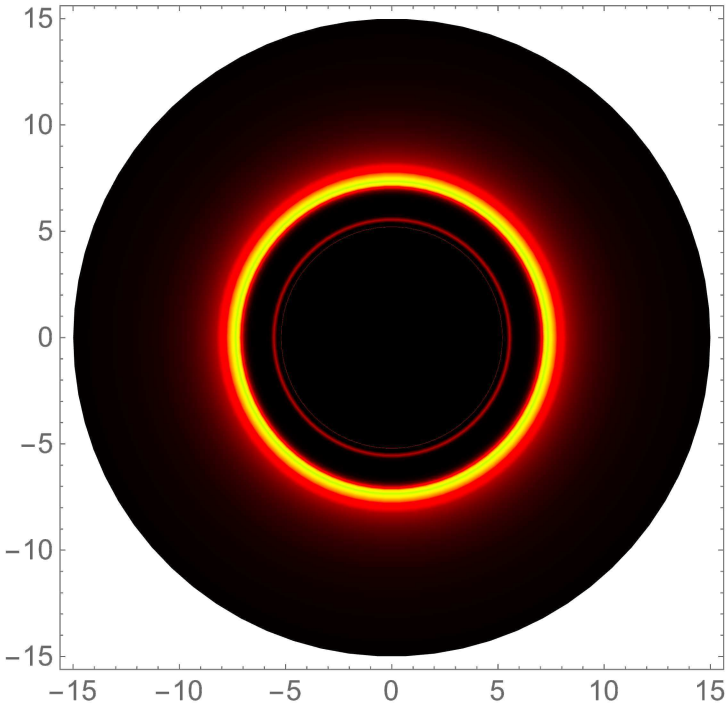

Figure 13 – Shadow of a Schwarzschild black hole considering the ISCO profile. The photon ring is barely visible as it only contribute to 3% of the imaging compared to the direct and lensed images.

4 CONCLUSIONS AND FINAL REMARKS

In this undergraduate thesis, we discussed and review how a single solution of general relativity led to a one hundred years of contribution by different into thinking on how could one observe black hole, or more precisely, its shadow.

Firstly, we made historical review in the introduction on how such a question was build through years of research. Then, at the second chapter, we went through the mathematical definition of black hole, derived the line element for the Schwarzschild spacetime, computed the geodesics within that spacetime, as well as how gravitational redshift alters signal transmission between two observers, and finally discussed the maximal analytical extension of the Schwarzschild black hole. Finally in chapter three, we correlated all that was derived for the geodesics in the Schwarzschild black hole for the process of shadowgraphy, namely, the computation of the shadow's size, the mapping between periastron radii and detection on the plate, in which many radius can be mapped to a impact parameter, so that then we computed the numerical simulation for the geodesics by integrating the angular equation in order to get information about the background geometry, so that in order to have the full characterization we only thing remaining was to have the optical and emission information of the accretion disk, which combined data treatments of the geodesics made possible to compute black hole shadow.

4.1 Observables

As pointed out by (FALCKE *et al.*, 2000), spherically symmetric inflows the trajectories converge to a single photon ring that exponentially approach the critical curve on the detector. As for either geometrically thin or thick disks the photon ring is broken into an infinite geometrical series contribution of exponentially demagnified self-similar rings generated by strongly lensed trajectories. However, the correlation of this fact to emission of a given intensity profile holds if and only if the emission of the disk is completely homogeneous, which in most astrophysical scenarios might seem as an utopia in the realm of approximations since quantities such as the flux ratio of the photon ring might vary according to the chosen intensity profile.

This is the step one in the attempt to measure photon rings by long baseline interferometry in astrophysical observations, since the $n = 0$ circuit is what the EHT measured, thus having no sufficient resolution for the photon ring. Hence, higher order circuit contributions up to $n = 2$ should be the main goal of future measurements.

Similarly to the analytical discussion by (PERLICK; TSUPKO, 2022), the shadow radius is actually unobservable given the fact that EHT is currently unable to measure any brightness bellow 10% of the peak luminosity with nowadays technology, which makes the angular size, at the current moment, a more suitable candidate for an observable quantity of the shadow's actual size.

4.2 Black Hole Mimickers

Even though this thesis is worried about reviewing probes to black hole shadow, a parallel line of work has been developed within this very same framework for observation of alternative ultra compact objects. Usually, one could consider objects that lie outside the range of general relativity and are only possible through modified theories of gravitation, or simply consider horizonless compact objects such as wormholes and gravastars, to probe theoretical and computational methods to see them in the sky. See (OLMO *et al.*, 2023; GUERRERO *et al.*, 2021b; GUERRERO *et al.*, 2022; ZENG *et al.*, 2022; ROSA; RUBIERA-GARCIA, 2022; ROSA, 2023).

REFERENCES

BAEZ, J. C.; BUNN, E. F. The meaning of einstein's equation. **American Journal of Physics**, American Association of Physics Teachers (AAPT), v. 73, n. 7, p. 644–652, jun. 2005. ISSN 1943-2909. Disponível em: http://dx.doi.org/10.1119/1.1852541.

CARROLL, S. M. **Spacetime and geometry**. [*S. l.*]: Cambridge University Press, 2019.

CHANDRASEKHAR, S. The mathematical theory of black holes. In: SPRINGER. **General Relativity and Gravitation: Invited Papers and Discussion Reports of the 10th International Conference on General Relativity and Gravitation, Padua, July 3–8, 1983**. [*S. l.*], 1984. p. 5–26.

COUDRAY, A.; NICOLAS, J.-P. Geometry of Vaidya spacetimes. **General Relativity and Gravitation**, v. 53, n. 8, p. 73, ago. 2021. ISSN 0001-7701, 1572-9532. Disponível em: https://link.springer.com/10.1007/s10714-021-02839-7.

CRISPINO, L. C. B.; LIMA, M. C. d. Expedição norte-americana e iconografia inédita de sobral em 1919. **Revista Brasileira de Ensino de Física**, SciELO Brasil, v. 40, n. 1, p. e1601, 2018.

D'INVERNO, R.; VICKERS, J. **Introducing Einstein's relativity: a deeper understanding**. [*S. l.*]: Oxford University Press, 2022.

EHT. First m87 event horizon telescope results. i. the shadow of the supermassive black hole. **The Astrophysical Journal Letters**, The American Astronomical Society, v. 875, n. 1, p. L1, 2019. Disponível em: https://dx.doi.org/10.3847/2041-8213/ab0ec7.

EHT. First m87 event horizon telescope results. ii. array and instrumentation. **The Astrophysical Journal Letters**, The American Astronomical Society, v. 875, n. 1, p. L2, 2019. Disponível em: https://dx.doi.org/10.3847/2041-8213/ab0c96.

EHT. First m87 event horizon telescope results. iii. data processing and calibration. v. 875, p. 3, 2019. Disponível em: https://iopscience.iop.org/article/10.3847/2041-8213/ab0c57.

EHT. First m87 event horizon telescope results. iv. imaging the central supermassive black hole. **The Astrophysical Journal Letters**, The American Astronomical Society, v. 875, n. 1, p. L4, 2019. Disponível em: https://dx.doi.org/10.3847/2041-8213/ab0e85.

EHT. First m87 event horizon telescope results. v. physical origin of the asymmetric ring. **The Astrophysical Journal Letters**, The American Astronomical Society, v. 875, n. 1, p. L5, 2019. Disponível em: https://dx.doi.org/10.3847/2041-8213/ab0f43.

EINSTEIN, A. Die feldgleichungen der gravitation. **Sitzungsberichte der Königlich Preußischen Akademie der Wissenschaften**, p. 844–847, 1915.

FALCKE, H.; MELIA, F.; AGOL, E. Viewing the Shadow of the Black Hole at the Galactic Center. **The Astrophysical Journal**, v. 528, n. 1, p. L13–L16, jan. 2000. ISSN 0004637X. Disponível em: https://iopscience.iop.org/article/10.1086/312423.

FUENTES, I. Lecture series on relativistic quantum information. In: **Diversities in Quantum Computation and Quantum Information**. [*S. l.*]: World Scientific, 2013. p. 107–147.

GENZEL. The nucleus of our galaxy. **Reports on Progress in Physics**, IOP Publishing, v. 57, n. 5, p. 417, 1994.

GENZEL. On the nature of the dark mass in the centre of the milky way. **Monthly Notices of the Royal Astronomical Society**, Blackwell Science Ltd Oxford, UK, v. 291, n. 1, p. 219–234, 1997.

GHEZ. The accelerations of stars orbiting the milky way's central black hole. **Nature**, Nature Publishing Group UK London, v. 407, n. 6802, p. 349–351, 2000.

GHEZ. The first measurement of spectral lines in a short-period star bound to the galaxy's central black hole: A paradox of youth. **The Astrophysical Journal**, v. 586, n. 2, p. L127, 2003. Disponível em: https://dx.doi.org/10.1086/374804.

GHEZ. Measuring distance and properties of the milky way's central supermassive black hole with stellar orbits. **The Astrophysical Journal**, IOP Publishing, v. 689, n. 2, p. 1044, 2008.

GRALLA, S. E.; HOLZ, D. E.; WALD, R. M. Black hole shadows, photon rings, and lensing rings. **Physical Review D**, v. 100, n. 2, p. 024018, jul. 2019. ISSN 2470-0010, 2470-0029. Disponível em: https://link.aps.org/doi/10.1103/PhysRevD.100.024018.

GRALLA, S. E.; LUPSASCA, A.; MARRONE, D. P. The shape of the black hole photon ring: A precise test of strong-field general relativity. **Physical Review D**, v. 102, n. 12, p. 124004, dez. 2020. ISSN 2470-0010, 2470-0029. Disponível em: https://link.aps.org/doi/10.1103/PhysRevD.102.124004.

GUERRERO, M.; OLMO, G. J.; RUBIERA-GARCIA, D. Double shadows of reflection-asymmetric wormholes supported by positive energy thin-shells. **Journal of Cosmology and Astroparticle Physics**, v. 2021, n. 04, p. 066, abr. 2021. ISSN 1475-7516. Disponível em: https://iopscience.iop.org/article/10.1088/1475-7516/2021/04/066.

GUERRERO, M.; OLMO, G. J.; RUBIERA-GARCIA, D.; GóMEZ, D. S.-C. Shadows and optical appearance of black bounces illuminated by a thin accretion disk. **Journal of Cosmology and Astroparticle Physics**, v. 2021, n. 08, p. 036, ago. 2021. ISSN 1475-7516. ArXiv:2105.15073 [gr-qc]. Disponível em: http://arxiv.org/abs/2105.15073.

GUERRERO, M.; OLMO, G. J.; RUBIERA-GARCIA, D.; GóMEZ, D. S.-C. Light ring images of double photon spheres in black hole and wormhole space-times. **Physical Review D**, v. 105, n. 8, p. 084057, abr. 2022. ISSN 2470-0010, 2470-0029. ArXiv:2202.03809 [gr-qc]. Disponível em: http://arxiv.org/abs/2202.03809.

HAWKING, S. W.; ELLIS, G. F. **The large scale structure of space-time**. [*S. l.*]: Cambridge university press, 2023.

LANDULFO, A. **Buracos negros:** rompendo os limites da ficção. [*S. l.*]: Editora Unesp, 2022.

LAPLACE, P.-S. de. **Exposition du système du monde**. [*S. l.*]: Bachelier, 1835.

LINDQUIST, R. W.; SCHWARTZ, R. A.; MISNER, C. W. Vaidya's Radiating Schwarzschild Metric. **Physical Review**, v. 137, n. 5B, p. B1364–B1368, mar. 1965. ISSN 0031-899X. Disponível em: https://link.aps.org/doi/10.1103/PhysRev.137.B1364.

LUMINET, J.-P. Image of a spherical black hole with thin accretion disk. **Astronomy and Astrophysics**, v. 75, p. 228–235, 1979. Disponível em: https://api.semanticscholar.org/CorpusID:117668975.

LUMINET, J.-P. Seeing Black Holes: From the Computer to the Telescope. **Universe**, v. 4, n. 8, p. 86, ago. 2018. ISSN 2218-1997. Disponível em: https://www.mdpi.com/2218-1997/4/8/86.

OLMO, G. J.; ROSA, J. L.; RUBIERA-GARCIA, D.; GóMEZ, D. S.-C. Shadows and photon rings of regular black holes and geonic horizonless compact objects. **Classical and Quantum Gravity**, v. 40, n. 17, p. 174002, set. 2023. ISSN 0264-9381, 1361-6382. ArXiv:2302.12064 [gr-qc]. Disponível em: http://arxiv.org/abs/2302.12064.

OPPENHEIMER, J. R.; SNYDER, H. On continued gravitational contraction. **Physical Review**, APS, v. 56, n. 5, p. 455, 1939.

PENROSE, R. Gravitational collapse and space-time singularities. **Physical Review Letters**, APS, v. 14, n. 3, p. 57, 1965.

PERLICK, V.; TSUPKO, O. Y. Calculating black hole shadows: Review of analytical studies. **Physics Reports**, v. 947, p. 1–39, fev. 2022. ISSN 03701573. Disponível em: https://linkinghub.elsevier.com/retrieve/pii/S0370157321003811.

POUND, R. V.; REBKA, G. A. Gravitational Red-Shift in Nuclear Resonance. **Physical Review Letters**, v. 3, n. 9, p. 439–441, nov. 1959. ISSN 0031-9007. Disponível em: https://link.aps.org/doi/10.1103/PhysRevLett.3.439.

POUND, R. V.; REBKA, G. A. Apparent Weight of Photons. **Physical Review Letters**, v. 4, n. 7, p. 337–341, abr. 1960. ISSN 0031-9007. Disponível em: https://link.aps.org/doi/10.1103/PhysRevLett.4.337.

ROSA, J. a. L. Observational properties of relativistic fluid spheres with thin accretion disks. **Phys. Rev. D**, American Physical Society, v. 107, p. 084048, Apr 2023. Disponível em: https://link.aps.org/doi/10.1103/PhysRevD.107.084048.

ROSA, J. a. L.; RUBIERA-GARCIA, D. Shadows of boson and proca stars with thin accretion disks. **Phys. Rev. D**, American Physical Society, v. 106, p. 084004, Oct 2022. Disponível em: https://link.aps.org/doi/10.1103/PhysRevD.106.084004.

ROVELLI, C. **General relativity:** the essentials. [*S. l.*]: Cambridge University Press, 2021.

SCHWARZSCHILD, K. **On the gravitational field of a mass point according to Einstein's theory**. 1999.

SYNGE, J. L. The Escape of Photons from Gravitationally Intense Stars. **Monthly Notices of the Royal Astronomical Society**, v. 131, n. 3, p. 463–466, fev. 1966. ISSN 0035-8711, 1365-2966. Disponível em: https://academic.oup.com/mnras/article-lookup/doi/10.1093/mnras/131.3.463.

THORNE, K. S.; WHEELER, J. A.; MISNER, C. W. **Gravitation**. [*S. l.*]: Freeman San Francisco, CA, 2000.

TONG, D. Lectures on general relativity. **DAMTP Cambridge**, 2013.

VAIDYA, P. C. Nonstatic Solutions of Einstein's Field Equations for Spheres of Fluids Radiating Energy. **Physical Review**, v. 83, n. 1, p. 10–17, jul. 1951. ISSN 0031-899X. Disponível em: https://link.aps.org/doi/10.1103/PhysRev.83.10.

WALD, R. M. **General relativity**. [*S. l.*]: University of Chicago Press, 1984.

WHEELER, J. A. **Geons, black holes and quantum foam:** a life in physics. [*S. l.*]: American Association of Physics Teachers, 2000.

ZENG, X.-X.; LI, G.-P.; HE, K.-J. The shadows and observational appearance of a noncommutative black hole surrounded by various profiles of accretions. **Nuclear Physics B**, v. 974, p. 115639, jan. 2022. ISSN 05503213. Disponível em: https://linkinghub.elsevier.com/retrieve/pii/S0550321321003369.

APPENDIX A – NOTATIONS AND CONVENTIONS

A.1 Units

Though the whole thesis we adopt the natural units system, which consists of $c = G = 1$ unless explicitly said in order to have clarifications. Physical quantities are said to have some power of ”mass dimension” or length dimension.

APPENDIX B – EXTRA THEOREMS AND PREPOSITIONS

For a more detailed discussion on the content of this appendix, see sasane2022mathematical, o1983semi, geroch2013differential, wald2010general.

B.1 Flows and Lie Derivative

Definition B.1 (Lie Derivative) *If $v^a \in \mathfrak{X}(\mathscr{M})$, the tensor derivation with respect to $\mathscr{L}_v$ is such that, the two properties need to be satisfied,*

$$\mathscr{L}_v(f) = v(f);\ \forall f \in \mathscr{F}; \tag{B.1}$$

$$\mathscr{L}_v x^b = [v^a, x^b].\forall x^a \in \mathfrak{X}(\mathscr{M}) \tag{B.2}$$

is called the Lie derivative relative to v^a.

This means that the Lie derivative of a scalar function reduces to the usual partial derivative and the Lie derivative of a vector field is often also called the Lie bracket.

One can easily prove that the Lie derivative satisfies the following properties.

(i) $\mathscr{L}_{av^b+bw^a} = a\mathscr{L}_v + b\mathscr{L}_w;\ a,b \in \mathbb{R}$.

(ii) $[\mathscr{L}_{\sqsubseteq}, \mathscr{L}_{\sqsupseteq}] = \mathscr{L}_{[v,w]}$.

(iii) $\mathscr{L}_v \mathrm{d}f = \mathrm{d}(v(f))$.

Definition B.2 (Integral Curves) *A curve $x^a = x^a(\lambda)$, is an integral curve of a smooth vector field, v^a, provided that $\frac{\mathrm{d}x^a}{\mathrm{d}\lambda} = v^a(p)$, such that $v^a(p)$ is a tangent vector at $p \in \mathscr{M}$.*

From the above definition, an integral curve is a solution of a first order differential equation, so it's a pretty straightforward name. Notice that given initial data, from ordinary differential equations theory, the integral curve of a vector field is unique.

Definition B.3 (Complete Vector Field) *A vector field, $v^a \in \mathfrak{X}(\mathscr{M})$ is said to be a complete vector field if each of its curves exists $\forall \lambda \in \mathbb{R}$.*

Thus, if manifold $\mathscr{M}$ admits a complete vector field, then for $p \in \mathscr{M}$, then there is a map for each frozen $\lambda \in \mathbb{R}$, ϕ_λ, such that,

$$p \overset{\phi_\lambda}{\longmapsto} x^a(\lambda) : \mathscr{M} \to \mathscr{M} \tag{B.3}$$

Which is a pretty straightforward definition. It states that if there is an ensemble of particles with different initial data and being transported along the vector field v^a and then just looking at a photograph at some frozen time t. We are now able to define the flow of a complete vector field.

Definition B.4 (Flow of Complete Vector Field) *Let $v^a \in \mathfrak{X}(\mathscr{M})$ be a complete vector field on $\mathscr{M}$ and $x^a : \mathbb{R} \to \mathscr{M}$ be the integral curve of v^a that satisfies the initial data, $x^a(0) = p \in \mathscr{M}$. For a real defined affine parameter λ, the map $\phi_\lambda : \mathscr{M} \to \mathscr{M}$, such that $\phi_\lambda(p) = x^a(\lambda) \forall p \in \mathscr{M}$, is said to be the flow map of the vector field v^a, and the collection, $\mathfrak{F}_v = \{\phi_\lambda : \mathscr{M} \to \mathscr{M}, \lambda \in \mathbb{R}\}$ is the flow of the vector field.*[1]

A important result from this definition is that the flow of a complete vector field is often also said to be a one-parameter group, since the map composition results in group operation on the set $\mathfrak{F}_v$.

B.2 Killing Vector Fields

Theorem B.1 (Killing Vector Field) *Let $(\mathscr{M}, g_{ab})$ be a manifold equipped with a metric and $\xi^a \in \mathfrak{X}(\mathscr{M})$ a complete vector field, with a defined flow ϕ_λ $\forall \lambda \in \mathbb{R}$. Then, ξ^a is a Killing vector field if and only if ϕ_λ is an isometry $\forall \lambda \in \mathbb{R}$.*

According to this theorem, then if $\phi_\lambda : \mathscr{M} \to \mathscr{M}$ is a one-parameter group of isometries, then the flow of ξ^a doesn't change the metric, i.e, $\phi_\lambda^* g_{ab} = g_{ab}$.

So if $\mathscr{L}_\xi T^{a_1 \ldots a_k}_{b_1 \ldots b_k} = 0$ is true globally, then ϕ_λ must be a symmetry transformation of $T^{a_1 \ldots a_k}_{b_1 \ldots b_k}$. Thus, the necessary and sufficient condition for ϕ_λ to be a group of isometries is $\mathscr{L}_\xi g_{ab} = 0$. Since, $\mathscr{L}_\xi g_{ab} = \nabla_a \xi_b + \nabla_b \xi_a$. Hence, the necessary and sufficient condition for ξ^a to be a Killing field is that it satisfies the Killing equation,

$$\nabla_a \xi_b + \nabla_b \xi_a = 0 \tag{B.4}$$

Proposition B.1 *If ξ^a is a Killing field, and x^a a geodesic with affine parameter $\lambda \in \mathbb{R}$, with tangent vector field u^a. Then $\xi_a u^a$ is constant along x^a.*

$$u^b \nabla_b (\xi_a u^a) = u^b u^a \nabla_b \xi_a + \xi_a u^b \nabla_b u^a = 0 \tag{B.5}$$

[1] Notice how the flow of a vector field is simply a family of diffeomorphisms.

The first term is zero because of Eq.B.4 and the second one is due to the geodesic equation.